Equilibration and aging of dense soft-sphere glass-forming liquids

Luis Enrique Sánchez-Díaz, Pedro Ramírez-González, and Magdaleno Medina-Noyola
Instituto de Física "Manuel Sandoval Vallarta," Universidad Autónoma de San Luis Potosí, Álvaro Obregón 64, 78000 San Luis Potosí, San Luis Potosí, México

(Received 1 December 2012; revised manuscript received 20 March 2013; published 22 May 2013)

The recently developed nonequilibrium extension of the self-consistent generalized Langevin equation theory of irreversible relaxation [Ramírez-González and Medina-Noyola, Phys. Rev. E **82**, 061503 (2010); **82**, 061504 (2010)] is applied to the description of the irreversible process of equilibration and aging of a glass-forming soft-sphere liquid that follows a sudden temperature quench, within the constraint that the local mean particle density remains uniform and constant. For these particular conditions, this theory describes the nonequilibrium evolution of the static structure factor $S(k;t)$ and of the dynamic properties, such as the self-intermediate scattering function $F_S(k,\tau;t)$, where τ is the correlation *delay* time and t is the *evolution* or *waiting* time after the quench. Specific predictions are presented for the deepest quench (to zero temperature). The predicted evolution of the α-relaxation time $\tau_\alpha(t)$ as a function of t allows us to define the *equilibration* time $t^{eq}(\phi)$, as the time after which $\tau_\alpha(t)$ has attained its equilibrium value $\tau_\alpha^{eq}(\phi)$. It is predicted that both, $t^{eq}(\phi)$ and $\tau_\alpha^{eq}(\phi)$, diverge as $\phi \to \phi^{(a)}$, where $\phi^{(a)}$ is the hard-sphere dynamic-arrest volume fraction $\phi^{(a)}$ ($\approx$0.582), thus suggesting that the measurement of *equilibrium* properties at and above $\phi^{(a)}$ is experimentally impossible. The theory also predicts that for fixed finite waiting times t, the plot of $\tau_\alpha(t;\phi)$ as a function of ϕ exhibits two regimes, corresponding to samples that have fully equilibrated within this waiting time ($\phi \leqslant \phi^{(c)}(t)$), and to samples for which equilibration is not yet complete ($\phi \geqslant \phi^{(c)}(t)$). The crossover volume fraction $\phi^{(c)}(t)$ increases with t but saturates to the value $\phi^{(a)}$.

DOI: 10.1103/PhysRevE.87.052306 PACS number(s): 82.70.Dd, 05.40.−a

I. INTRODUCTION

Classical and statistical thermodynamics deal with the equilibrium states of matter [1,2]. Driving the system from one equilibrium state to another, however, involves the passage of the system through a sequence of instantaneous states that do not satisfy the conditions for thermodynamic equilibrium and, hence, constitute a nonequilibrium process [3,4]. The description of these processes fall outside the realm of classical and statistical thermodynamics, unless the sequence of nonequilibrium states do not depart appreciably from a sequence of equilibrium states. Such an idealized process can be thought of as an infinite sequence of infinitesimally small changes in the driving control parameter, after each of which the system is given sufficient time to equilibrate. This so-called quasistatic process is an excellent representation of real process when the equilibration times of the system are sufficiently short. However, when the equilibration kinetics is very slow, virtually any change will involve intrinsically nonequilibrium states whose fundamental understanding must unavoidably be done from the perspective of a nonequilibrium theory [5].

These concepts become particularly relevant for the description of the slow dynamics of metastable glass-forming liquids in the vicinity of the glass transition [6,7]. It is well known that the decay time of the slowest relaxation processes (the so-called α-relaxation time τ_α) increases without bound as the temperature T is lowered below the glass transition temperature T_g. It is then natural to think that the *equilibration* time of the system must also increase accordingly. To be more precise, let us imagine that a glass-forming liquid, initially at an arbitrary temperature $T^{(i)}$, is suddenly cooled at time $t = 0$ to a final temperature T, after which it is allowed to evolve spontaneously toward its thermodynamic equilibrium state. Imagine that we then monitor its α-relaxation time $\tau_\alpha(t)$ as a function of the evolution or "waiting" time t elapsed after the quench. We say that the system has equilibrated when $\tau_\alpha(t)$ reaches the plateau that defines its final equilibrium value $\tau_\alpha^{eq}(T)$, which must only depend on the final temperature T. The beginning of this plateau occurs at a certain value of the waiting time t, which we refer to as the *equilibration* time $t^{eq}(T)$; this equilibration time must also depend on the final temperature T.

There are indications from recent computer simulation experiments [8,9] that in the metastable regime these two characteristic times, $\tau_\alpha^{eq}(T)$ and $t^{eq}(T)$, are related to each other as $t^{eq}(T) \propto [\tau_\alpha^{eq}(T)]^\eta$, with an exponent $\eta \gtrsim 1$. This implies that in order to measure the actual equilibrium value $\tau_\alpha^{eq}(T)$ we have to wait, before starting the measurement of $\tau_\alpha^{eq}(T)$, for an equilibration time $t^{eq}(T)$ that will increase essentially as fast as $\tau_\alpha^{eq}(T)$ itself. This poses an obvious practical problem for the measurement of $\tau_\alpha^{eq}(T)$ when the temperature T approaches the glass transition temperature T_g, since sooner or later we shall be unable to wait this required equilibration time. This situation then implies that it is impossible to discard a scenario in which the *equilibrium* α-relaxation time $\tau_\alpha^{eq}(T)$ diverges at a singular temperature $T^{(a)}$, since the equilibration time $t^{eq}(T)$ needed to observe this divergence will also diverge at that temperature; i.e., it will be impossible to equilibrate the system at a final temperature near or below $T^{(a)}$ within experimental waiting times. Of course, a measurement carried out at a finite t, will always report a result for τ_α, but this result will correspond to $\tau_\alpha(t)$, the nonequilibrium value of the α-relaxation time registered at that waiting time t. Thus, the analysis of these experimental measurements cannot be based on the postulate that the system has reached equilibrium; instead, one needs to interpret these experiments in the framework of a quantitative theory of slowly relaxing nonequilibrium processes.

Until recently, however, no *quantitative, first-principles* theory had been developed and applied to describe the slow *nonequilibrium* relaxation of *structural* glass-forming atomic or colloidal liquids. About a decade ago Latz [10] attempted to extend the conventional mode coupling theory (MCT) of the ideal glass transition [11–14], to describe the aging of suddenly quenched glass-forming liquids. A major aspect of his work involved the generalization to nonequilibrium conditions of the conventional equilibrium projection operator approach [15] to derive the corresponding memory function equations in which the mode coupling approximations could be introduced. Similarly, De Gregorio *et al.* [16] discussed time-translational invariance and the fluctuation-dissipation theorem in the context of the description of slow dynamics in system out of equilibrium but close to dynamical arrest. They also proposed extensions of approximations long known within MCT. Unfortunately, in neither of these theoretical efforts were quantitative predictions presented that could be contrasted with experimental or simulated results in specific model systems of *structural* glass formers.

In an independent but similarly aimed effort, on the other hand, the self-consistent generalized Langevin equation (SCGLE) theory of colloid dynamics [17–20] and of dynamic arrest [21–25] has recently been extended to describe the (nonequilibrium) spatially nonuniform and temporally nonstationary evolution of glass-forming colloidal liquids. Such an extension was introduced and described in detail in Ref. [26] and will be referred to as the *nonequilibrium* self-consistent generalized Langevin equation (NE-SCGLE) theory. As one can imagine, the number and variety of the phenomena that could be studied with this new theory may be enormous, and to start its systematic application we must focus on simple classes of physically relevant conditions. Thus, as a first simple illustrative application, this theory was applied in Ref. [27] to a model colloidal liquid with hard-sphere plus short-ranged attractive interactions suddenly quenched to an attractive glass state.

The aim of the present work is to start a systematic exploration of the scenario predicted by this theory when applied to the simplest irreversible processes in the simplest and best-defined model system. In the present case we refer to the irreversible isochoric evolution of a glass-forming liquid of particles interacting through purely repulsive soft-sphere interactions, initially at a fluidlike state, whose temperature is suddenly quenched to a final value $T^{(f)} = 0$, at which the expected equilibrium state is that of a hard-sphere liquid at volume fraction ϕ. Such a process mimics the spontaneous search for the equilibrium state of this hard-sphere liquid, driven to nonequilibrium conditions by some perturbation (shear, for example, [28,29]), which ceases at a time $t = 0$. One possibility is that the system will recover its equilibrium state within an equilibration time $t^{eq}(\phi)$ that depends on the fixed volume fraction ϕ. The other possibility is that the system ages forever in the process of becoming a glass. The application of the NE-SCGLE theory to these irreversible processes results in a well-defined scenario of the spontaneous nonequilibrium response of the system, whose main features are explained and illustrated in this paper.

In the following section we provide a brief summary of the NE-SCGLE theory, appropriately written to describe the equilibration of a monocomponent glass-forming liquid constrained to remain spatially uniform. Section III defines the specific model to which this theory will be applied, discusses the strategy of solution of the resulting equations, and illustrates the main features of the results. Section IV presents the scenario predicted by the NE-SCGLE theory for the first possibility mentioned above, namely, that the system is able to reach its thermodynamic equilibrium state. In this case we find that the equilibrium α-relaxation time $\tau_\alpha^{eq}(\phi)$ and the equilibration time $t^{eq}(\phi)$ needed to reach it will remain finite for volume fractions smaller than a critical value $\phi^{(a)}$, but that both characteristic times will diverge as ϕ approaches this dynamic-arrest volume fraction $\phi^{(a)} \approx 0.582$ and will remain infinite for $\phi \geqslant \phi^{(a)}$. Although it is intrinsically impossible to witness the actual predicted divergence, the theory makes distinct predictions regarding the transient nonequilibrium evolution occurring within experimentally reasonable waiting times t.

In Sec. V we analyze the complementary regime, $\phi \geqslant \phi^{(a)}$, in which the system, rather than reaching equilibrium within finite waiting times, is predicted to age forever. In this regime we find that the long-time asymptotic limit of $S(k;t)$ will no longer be the expected equilibrium static structure factor $S^{(eq)}(k)$, but another, nonequilibrium but well-defined, static structure factor, which we denote as $S^{(a)}(k)$ and which depends on the protocol of the quench. Furthermore, contrary to the kinetics of the equilibration process, in which $S(k;t)$ approaches $S^{(eq)}(k)$ in an exponential-like fashion, this time the decay of $S(k;t)$ to its asymptotic value $S^{(a)}(k)$ follows a much slower power law.

In Sec. VI we put together the two regimes just described, in an integrated picture, which outlines the predicted scenario for the crossover from equilibration to aging. There we find that the discontinuous and singular behavior underlying the previous scenario is intrinsically unobservable, due to the finiteness of the experimental measurements, which constrains the observations to finite time windows. This practical but fundamental limitation converts the discontinuous dynamic arrest transition into a blurred crossover, strongly dependent on the protocol of the experiment and of the measurements.

The main purpose of the present paper is to explain in sufficient detail the methodological aspects of the application of the theory, so as to serve as a reliable reference for the eventual application of this nonequilibrium theory to the same system but with different nonequilibrium processes (e.g., different quench protocols) or, in general, to different systems and processes. Thus, we do not report here the results of the systematic quantitative comparison of the scenario explained here with available specific simulations or experiments, which are being reported separately. Thus, the final section of the paper briefly refers to the main features of those comparisons and discusses possible directions for further work.

II. REVIEW OF THE NE-SCGLE THEORY

Let us mention that the referred NE-SCGLE theory derives from a nonequilibrium extension of Onsager's theory of thermal fluctuations [26], and it consists of the time evolution equations for the mean value $\overline{n}(\mathbf{r},t)$ and for the covariance $\sigma(\mathbf{r},\mathbf{r}';t) \equiv \overline{\delta n(\mathbf{r},t)\delta n(\mathbf{r}',t)}$ of the fluctuations

$\delta n(\mathbf{r},t) = n(\mathbf{r},t) - \overline{n}(\mathbf{r},t)$ of the local concentration profile $n(\mathbf{r},t)$ of a colloidal liquid. These two equations are coupled, through a local mobility function $b(\mathbf{r},t)$, with the two-time correlation function $C(\mathbf{r},\mathbf{r}';t,t') \equiv \overline{\delta n(\mathbf{r},t)\delta n(\mathbf{r}',t')}$. A set of well-defined approximations on the memory function of $C(\mathbf{r},\mathbf{r}';t,t')$, detailed in Ref. [26], results in the referred NE-SCGLE theory.

As discussed in Ref. [26], for given interparticle interactions and applied external fields, the NE-SCGLE self-consistent theory is, in principle, able to describe the evolution of a liquid from an initial state with arbitrary mean and covariance $\overline{n}^0(\mathbf{r})$ and $\sigma^0(\mathbf{r},\mathbf{r}')$, towards its equilibrium state characterized by the equilibrium local concentration profile $\overline{n}^{eq}(\mathbf{r})$ and equilibrium covariance $\sigma^{eq}(\mathbf{r},\mathbf{r}')$. These equations are, in principle, quite general and contain well-known theories as particular limits. For example, ignoring certain memory function effects, the evolution equation for the mean profile $\overline{n}(\mathbf{r},t)$ becomes the fundamental equation of dynamic density functional theory [30], whereas the "conventional" equilibrium SCGLE theory [23] (analogous in most senses to MCT [11]) is recovered when full equilibration is assumed and spatial heterogeneities are suppressed. The NE-SCGLE theory, however, provides a much more general theoretical framework, which, in principle, describes the spatially heterogeneous and temporally nonstationary evolution of a liquid toward its ordinary stable thermodynamic equilibrium state. This state, however, will become unreachable if well-defined dynamic arrest conditions arise along the equilibration pathway, in which case the system evolves towards a distinct and predictable dynamically arrested state through an evolution process that involves aging as an essential feature.

To start the systematic application of this general theory to more specific phenomena we must focus on a simple class of physical conditions. Thus, let us consider the irreversible evolution of the structure and dynamics of a system *constrained* to suffer a programmed process of spatially *homogeneous* compression or expansion (and/or of cooling or heating). Under these conditions, rather than solving the time-evolution equation for $\overline{n}(\mathbf{r};t)$, we assume that the system is constrained to remain *spatially uniform*, $\overline{n}(\mathbf{r};t) = \overline{n}(t)$, according to a *prescribed* time dependence $\overline{n}(t)$ of the uniform bulk concentration and/or to a prescribed uniform time-dependent temperature $T(t)$. Among the many possible programmed protocols ($\overline{n}(t)$, $T(t)$) that one could devise to drive or to prepare the system, in this paper we restrict ourselves to one of the simplest and most fundamental protocols, which corresponds to the limit in which the system, initially at an equilibrium state determined by initial values of the control parameters, $(\overline{n}^{(i)},T^{(i)})$, must adjust itself in response to a sudden and instantaneous change of these control parameters to new values $(\overline{n}^{(f)},T^{(f)})$, according to the "program" $\overline{n}(t) = \overline{n}^{(i)}\theta(-t) + \overline{n}^{(f)}\theta(t)$ and $T(t) = T^{(i)}\theta(-t) + T^{(f)}\theta(t)$, with $\theta(t)$ being Heaviside's step function. Furthermore, just like in the first illustrative example described in Ref. [27], here we also restrict ourselves to the description of an even simpler subclass of irreversible processes, namely, the isochoric cooling or heating of the system, in which its number density is constrained to remain constant, i.e., $\overline{n}(t) = \overline{n}^{(i)} = \overline{n}^{(f)} = \overline{n}$, while the temperature $T(t)$ changes abruptly from its initial constant value $T^{(i)}$ to a final constant value $T^{(f)}$ at $t = 0$.

Under conditions of spatial uniformity, $C(\mathbf{r},\mathbf{r}';t,t')$ can be written as

$$C(|\mathbf{r}-\mathbf{r}'|,t'-t;t) = \frac{\overline{n}}{(2\pi)^3}\int d\mathbf{k}\exp[-i\mathbf{k}\cdot(\mathbf{r}-\mathbf{r}')]F(k,\tau;t), \quad (2.1)$$

with $\tau \equiv (t'-t) \geqslant 0$, and where $F(k,\tau;t)$ is the t-evolving nonequilibrium intermediate scattering function (NE-ISF). Similarly, the covariance $\sigma(\mathbf{r},\mathbf{r}';t)$ can be written as

$$\sigma(|\mathbf{r}-\mathbf{r}'|;t) = \frac{\overline{n}}{(2\pi)^3}\int d\mathbf{k}\exp[-i\mathbf{k}\cdot(\mathbf{r}-\mathbf{r}')]S(k;t), \quad (2.2)$$

with $S(k;t) \equiv F(k,\tau=0;t)$ being the time-evolving static structure factor. Under these conditions, the NE-SCGLE theory determines that the time-evolution equation for the covariance (Eq. (2.11) of Ref. [27]) may be written as an equation for $S(k;t)$ which, for $t > 0$, reads

$$\frac{\partial S(k;t)}{\partial t} = -2k^2 D^0 b(t)\overline{n}^{(f)}\mathcal{E}^{(f)}(k)[S(k;t) - 1/\overline{n}\mathcal{E}^{(f)}(k)]. \quad (2.3)$$

In this equation the function $\mathcal{E}^{(f)}(k) = \mathcal{E}(k;\overline{n},T^{(f)})$ is the Fourier transform (FT) of the functional derivative $\mathcal{E}[|\mathbf{r}-\mathbf{r}'|;n,T] \equiv [\delta\beta\mu[\mathbf{r};n]/\delta n(\mathbf{r}')]$, evaluated at $n(\mathbf{r}) = \overline{n}$ and $T = T^{(f)}$. As discussed in Refs. [26,27], this thermodynamic object embodies the information, assumed known, of the chemical equation of state, i.e., of the functional dependence of the electrochemical potential $\mu[\mathbf{r};n]$ on the number density profile $n(\mathbf{r})$.

The solution of this equation, for arbitrary initial condition $S(k;t=0) = S^{(i)}(k)$, can be written as

$$S(k;t) = S^{(i)}(k)e^{-\alpha(k)u(t)} + [\overline{n}\mathcal{E}^{(f)}(k)]^{-1}(1 - e^{-\alpha(k)u(t)}), \quad (2.4)$$

with

$$\alpha(k) \equiv 2k^2 D^0 \overline{n}\mathcal{E}^{(f)}(k), \quad (2.5)$$

and with

$$u(t) \equiv \int_0^t b(t')dt'. \quad (2.6)$$

In the equations above, the time-evolving mobility $b(t)$ is defined as $b(t) \equiv D_L(t)/D^0$, with D^0 being the short-time self-diffusion coefficient and $D_L(t)$ the long-time self-diffusion coefficient at evolution time t. As explained in Refs. [26] and [27], the equation

$$b(t) = \left[1 + \int_0^\infty d\tau\,\Delta\zeta^*(\tau;t)\right]^{-1} \quad (2.7)$$

relates $b(t)$ with the t-evolving, τ-dependent friction coefficient $\Delta\zeta^*(\tau;t)$ given approximately by

$$\Delta\zeta^*(\tau;t) = \frac{D_0}{24\pi^3\overline{n}}\int d\mathbf{k}\,k^2\left[\frac{S(k;t)-1}{S(k;t)}\right]^2 \times F(k,\tau;t)F_S(k,\tau;t). \quad (2.8)$$

Thus, the presence of $b(t)$ in Eq. (2.6) couples the formal solution for $S(k;t)$ in Eq. (2.4) with the solution of the

nonequilibrium version of the SCGLE equations for the collective and self NE-ISFs $F(k,\tau;t)$ and $F_S(k,z;t)$. These equations are written, in terms of the Laplace transforms (LTs) $F(k,z;t)$ and $F_S(k,\tau;t)$, as

$$F(k,z;t) = \frac{S(k;t)}{z + \frac{k^2 D^0 S^{-1}(k;t)}{1+\lambda(k)\ \Delta\zeta^*(z;t)}} \tag{2.9}$$

and

$$F_S(k,z;t) = \frac{1}{z + \frac{k^2 D^0}{1+\lambda(k)\ \Delta\zeta^*(z;t)}}, \tag{2.10}$$

with $\lambda(k)$ being a phenomenological "interpolating function" [23], given by

$$\lambda(k) = 1/[1 + (k/k_c)^2], \tag{2.11}$$

with $k_c = 1.118 \times k_{\max}(t)$, where $k_{\max}(t)$ is the position of the main peak of $S(k;t)$. The simultaneous solution of Eqs. (2.3)–(2.10) above, constitute the NE-SCGLE description of the spontaneous evolution of the structure and dynamics of an *instantaneously* and *homogeneously* quenched liquid.

Of course, one important aspect of this analysis refers to the possibility that along the process the system happens to reach the condition of dynamic arrest. For the discussion of this important aspect it is useful to consider the long-τ (or small-z) asymptotic stationary solutions of Eqs. (2.8) and (2.9), the so-called nonergodicity parameters, which are given by [26]

$$f(k;t) \equiv \lim_{\tau\to\infty} \frac{F(k,\tau;t)}{S(k)} = \frac{\lambda(k;t)S(k;t)}{\lambda(k;t)S(k;t) + k^2\gamma(t)} \tag{2.12}$$

and

$$f_S(k;t) \equiv \lim_{\tau\to\infty} F_S(k,\tau;t) = \frac{\lambda(k;t)}{\lambda(k;t) + k^2\gamma(t)}, \tag{2.13}$$

where the t-dependent squared localization length $\gamma(t)$ is the solution of

$$\frac{1}{\gamma(t)} = \frac{1}{6\pi^2\overline{n}^{(f)}} \int_0^\infty dk k^4 \times \frac{[S(k;t)-1]^2\lambda^2(k;t)}{[\lambda(k;t)S(k;t) + k^2\gamma(t)][\lambda(k;t) + k^2\gamma(t)]}. \tag{2.14}$$

Notice also that these equations are the nonequilibrium extension of the corresponding results of the equilibrium SCGLE theory (referred to as the "bifurcation equations" in the context of MCT [11]), and their derivation from Eqs. (2.8)–(2.10) follows the same arguments as in the equilibrium case [18]. The solution $\gamma(t)$ of Eq. (2.14) and the mobility $b(t)$ constitute two complementary dynamic order parameters, in the sense that if $\gamma(t)$ is finite [or $b(t) = 0$], then the system must be considered dynamically arrested at that waiting time t, whereas if $\gamma(t)$ is infinite, then the particles retain a finite mobility, $b(t) > 0$, and the instantaneous state of the system is ergodic or fluidlike.

We recall that the first relevant application of Eq. (2.14) is the determination of the *equilibrium* dynamic arrest diagram in control-parameter space [which, in the present case, is the density-temperature plane (n,T)]. This diagram determines the region of fluidlike states, for which the solution $\gamma^{eq}(n,T)$ [of Eq. (2.14), with $S(k;t) = S^{eq}(k;n,T)$] is infinite. The complementary region contains the dynamically arrested states, for which $\gamma^{eq}(n,T)$ is finite. The borderline between these two regions is the dynamic arrest transition line. Due to the complementarity of the dynamic order parameters $\gamma(t)$ and $b(t)$, this curve is also the borderline between the region where the mobility $b(t)$ will reach its equilibrium value, $\lim_{t\to\infty} b(t) = b^{eq}(n,T) \geqslant 0$, and the region of arrested states, where $\lim_{t\to\infty} b(t) = 0$. Thus, since $b^{eq}(n,T) = D^*(n,T) \equiv D_L(n,T)/D^0$, where $D_L(n,T)$ is the equilibrium long-time self-diffusion coefficient at the point (n,T), this line is also the isodiffusivity curve corresponding to $D^* = 0$.

Let us end this summary by noticing that the NE-SCGLE theory was originally developed having in mind a system with underlying Brownian (not molecular) dynamics, in which the Brownian particles diffuse between collisions with a constant free-diffusion coefficient D^0. This is the value of $D_L(n,T)$ in the absence of interparticle interactions. Thus, it is natural to scale $D_L(n,T)$ with D^0 to define the dimensionless long-time self-diffusion coefficient $D^*(n,T) \equiv D_L(n,T)/D^0$. As recently demonstrated [31,32], however, this is also an adequate scaling for atomic liquids provided that D^0 is given by its kinetic-theory value. In fact, this scaling is instrumental in appreciating the precise long-time dynamic equivalence between Brownian and atomic liquids, discussed in these two references and summarized, for example, in Fig. 2 of Ref. [32]. The corresponding scaling for the structural α relaxation time τ_α is $\tau^* \equiv k^2 D^0 \tau_\alpha$.

III. GENERAL FEATURES OF THE SOLUTION AND A SPECIFIC ILLUSTRATION

Let us now discuss some general features of the solution of the NE-SCGLE equations just presented. This discussion has a general character, but for the sake of clarity we illustrate the main concepts in the context of one specific application. Thus, consider a monocomponent fluid of soft spheres of diameter σ, whose particles interact through the truncated Lennard-Jones (TLJ) pair potential (also referred to as Weeks-Chandler-Andersen potential [33]), which vanishes for $r \geqslant \sigma$, but which for $r \leqslant \sigma$ is given, in units of the thermal energy $k_B T = \beta^{-1}$, by

$$\beta u(r) = \epsilon\left[\left(\frac{\sigma}{r}\right)^{2\nu} - 2\left(\frac{\sigma}{r}\right)^{\nu} + 1\right]. \tag{3.1}$$

The state space of this system is spanned by the volume fraction $\phi = \pi\overline{n}\sigma^3/6$ and the reduced temperature $T^* \equiv k_B T/\epsilon$.

A. Thermodynamic framework: Local curvature of the free energy surface

In order to apply Eqs. (2.3)–(2.10) to this model system, we first need to determine its thermodynamic property $\mathcal{E}^{(f)}(k)$. As indicated above, this is the FT of the functional derivative $\mathcal{E}[|\mathbf{r}-\mathbf{r}'|;n,T] \equiv [\delta\beta\mu[\mathbf{r};n]/\delta n(\mathbf{r}')]$, which can also be written as $\mathcal{E}[|\mathbf{r}-\mathbf{r}'|;n,T] = \delta(\mathbf{r}-\mathbf{r}')/\overline{n} - c(|\mathbf{r}-\mathbf{r}'|;n,T)$, with $c(r;n,T)$ being the ordinary direct correlation function [2]. This is an intrinsically thermodynamic property, related with the *equilibrium* static structure factor $S^{(eq)}(k;\overline{n},T)$ by the Ornstein-Zernike (OZ) equation, which in Fourier space reads $\overline{n}\mathcal{E}(k;\overline{n},T)S^{(eq)}(k;\overline{n},T) = 1$. The OZ equation is the basis for the construction of the approximate integral equations of the

equilibrium statistical thermodynamics of liquids [2]. In fact, we employ one such approximation to determine $\overline{n}\mathcal{E}(k;\overline{n},T)$ for our soft-sphere system as $\overline{n}\mathcal{E}(k;\overline{n},T) = 1/S^{(eq)}(k;\overline{n},T)$, in which we approximate the equilibrium static structure factor $S^{(eq)}(k;\overline{n},T)$ by its Percus-Yevick/Verlet-Weis (PY-VW) approximation [33–35], $S^{(eq)}(k\sigma;\phi,T^*,\nu) \approx S^{(PY\text{-}VW)}(k\sigma;\phi,T^*,\nu) \equiv S_{HS}^{(PY\text{-}VW)}(\lambda k\sigma;\lambda^3\phi)$, with the effective hard-sphere diameter $\lambda \equiv \sigma_{HS}(T^*,\nu)/\sigma$ determined by the blip function method [36] as $\lambda(T^*,\nu) = \{1 - 3\int_0^1 dx x^2 \exp[-\frac{1}{T^*}(\frac{1}{x^{2\nu}} - \frac{2}{x^{\nu}} + 1)]\}^{1/3}$. The function $S_{HS}^{(PY\text{-}VW)}(k\sigma;\phi)$ is the PY-VW static structure factor of the fluid of hard spheres of diameter σ and volume fraction ϕ, i.e., $S_{HS}^{(PY\text{-}VW)}(k\sigma;\phi) \equiv S^{(PY)}(\lambda_w k\sigma;\phi_w)$, with $\phi_w \equiv \phi - \phi^2/16$ and $\lambda_w \equiv (\phi_w/\phi)^{1/3}$, and with the function $S^{(PY)}(k\sigma;\phi)$ being the solution of the OZ equation with Percus-Yevick closure for the same HS fluid.

Let us emphasize that for the present purpose, approximations such as these must be regarded solely as a practical and approximate mean to determine the thermodynamic property $\overline{n}\mathcal{E}(k;\overline{n},T)$, which is essentially the local curvature of the free energy surface at the state point $(\overline{n},T)$ [26,37]. This property directly determines the *equilibrium* structure factor $S^{(eq)}(k;\overline{n},T)$ through the equilibrium relationship $\overline{n}\mathcal{E}(k;\overline{n},T)S^{(eq)}(k;\overline{n},T) = 1$, and in practice we actually use this relationship to determine $\overline{n}\mathcal{E}(k;\overline{n},T)$. The main message of Eq. (2.3), however, is that the experimentally observable, nonequilibrium, static structure factor $S(k;t)$ is not determined by any OZ equilibrium condition, but by Eq. (2.3) itself, with the thermodynamic property $\overline{n}\mathcal{E}(k;\overline{n},T)$ driving the nonequilibrium evolution in the manner indicated by its explicit appearance in this equation.

B. Thermodynamic equilibrium vs dynamically arrested states

In what follows, we are interested in studying the scenario revealed by the solution $S(k;t)$ of Eq. (2.3), for the process of isochoric equilibration (or lack of equilibration) of the static structure of a system subjected to a temperature control protocol $T(t) = T^{(i)}\theta(-t) + T^{(f)}\theta(t)$, corresponding to an instantaneous temperature quench to a final temperature $T^{(f)}$ denoted simply as T. Thus, the system is assumed to be prepared at an initial equilibrium homogeneous state characterized by a bulk particle number density $\overline{n}$ and temperature $T^{(i)}$, at which its initial static structure factor is $S(k;t=0) = S^{(i)}(k)$. Upon suddenly changing the temperature of this system to the new value T, one normally expects that the system will reach full thermodynamic equilibrium, i.e., that the long-time asymptotic limit of $S(k;t)$ will be the equilibrium static structure factor $S^{(eq)}(k;\overline{n},T) = 1/\overline{n}\mathcal{E}(k;\overline{n},T)$. According to Eq. (2.3), reaching this value is also a sufficient condition for $S(k;t)$ to reach a *stationary* state.

According to the same equation, however, this is *not a necessary* condition for the stationarity of $S(k;t)$, which could also be attained if $\lim_{t\to\infty} b(t) = 0$, even in the absence of thermodynamic equilibrium [i.e., even if $\lim_{t\to\infty} S(k;t) \neq 1/\overline{n}\mathcal{E}(k;\overline{n},T)$]. If the long-time stationary state attained is the thermodynamic equilibrium state, we say that the system is ergodic at the point $(\overline{n},T)$. The second condition, in contrast, corresponds to dynamically arrested states, in which the long-time asymptotic limit of $S(k;t)$ might differ from the expected thermodynamic equilibrium value $S^{(eq)}(k;\overline{n},T) = 1/\overline{n}\mathcal{E}(k;\overline{n},T)$. Clearly, these are two mutually exclusive and fundamentally different classes of possible stationary states which can only be distinguished if we know the long-time limit of $b(t)$. This is, however, not a thermodynamic property, and, hence, the discrimination of the ergodic or nonergodic nature of the state point $(\overline{n},T)$ must be based on a dynamic or transport theory that allows the determination of $b(t)$.

One such theory is precisely the SCGLE theory: To decide if the long-time stationary state corresponding to the point $(\overline{n},T)$ will be an ergodic or an arrested state one can use the equilibrium static structure factor $S^{(eq)}(k;\overline{n},T)$ in Eq. (2.14) to calculate $\gamma^{(eq)}(\overline{n},T)$. If the solution is infinite, we say that the asymptotic stationary state is ergodic and, hence, that at the point $(\overline{n},T)$ the system will be able to reach its thermodynamic equilibrium state without impediment, so that $\lim_{t\to\infty} S(k;t) = 1/\overline{n}\mathcal{E}(k;\overline{n},T)$. On the other hand, if the solution for $\gamma^{(eq)}(\overline{n},T)$ turns out to be finite, this means that the system will become dynamically arrested and that the long-time limit of $S(k;t)$ at the point $(\overline{n},T)$ will not necessarily be its thermodynamic equilibrium value $S^{(eq)}(k;\overline{n},T) = 1/\overline{n}\mathcal{E}(k;\overline{n},T)$. Instead, we shall have that $\lim_{t\to\infty} S(k;t) = S^{(a)}(k)$, with a truly nonequilibrium structure factor $S^{(a)}(k)$, different from $S^{(eq)}(k;\overline{n},T)$ and obtained as an alternative stationary solution of Eq. (2.3). In this manner, by calculating $\gamma^{(eq)}(\overline{n},T)$ at all state points $(\overline{n},T)$ one can scan the state space to determine the region of dynamically arrested states of the system.

We have employed in this manner the PY-VW approximation for the equilibrium static structure factor $S^{(eq)}(k;\overline{n},T)$ of the TLJ soft-sphere model, to determine the region of its fluidlike ergodic states and the region of its dynamically arrested states. The resulting dynamic arrest transition line is represented by the solid curve in Fig. 1 for the TLJ

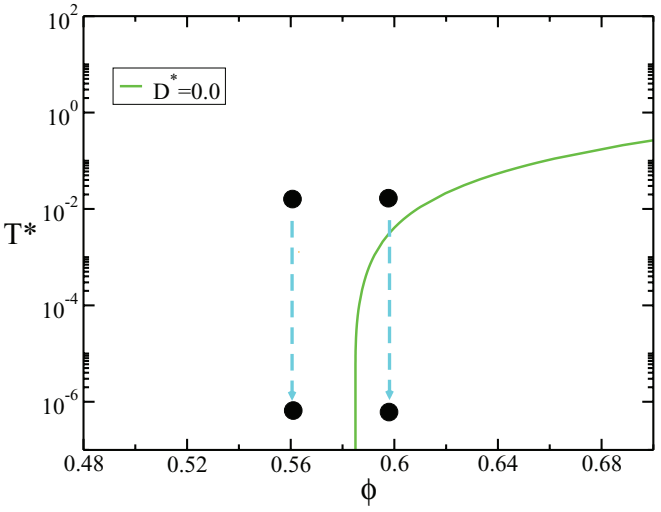

FIG. 1. (Color online) Dynamic arrest line (or isodiffusivity curve with $D^* = 0$) in the (ϕ,T^*) state space of the TLJ fluid, Eq. (3.1), with $\nu = 6$. The vertical downward arrows represent two fundamentally different classes of irreversible isochoric processes. In the first case, the fixed volume fraction ϕ is smaller than the dynamic arrest volume fraction $\phi^{(a)}$ (=0.582), whereas in the second ϕ is larger than $\phi^{(a)}$.

fluid with $\nu = 6$, whose $T^* \to 0$ limit coincides with the dynamic arrest volume fraction $\phi^{(a)}$ of the hard-sphere liquid, predicted to occur at $\phi^{(a)} = 0.582$ [8]. As indicated in the figure (and as explained at the end of the previous section), this transition line is also the isodiffusivity curve corresponding to $D^* = 0$. In addition, as demonstrated in Ref. [38], it is also an isostructural curve, as well as an iso-ϕ_{HS} curve [corresponding to $\phi_{HS}(\phi, T^*) = \phi_{HS}^{(a)} \approx 0.582$]. Hence, one manner to derive an equation that describes this dynamic arrest curve is to write the equation for the iso-ϕ_{HS} curve corresponding to $\phi_{HS}(\phi, T^*) = \phi_{HS}^{(a)}$. This can be done rather easily in the low-temperature limit, in which, according to [38], for the TLJ model $\phi_{HS}(\phi, T^*)$ may be approximated by the blip-function method, yielding $\phi_{HS}(\phi, T^*) \approx \phi[1 - (3\sqrt{\pi}/2\nu)\sqrt{T^*}]$. Thus, the iso-$\phi_{HS}$ curve corresponding to $\phi_{HS}^{(a)}$ is described at low temperatures by $T^{*(a)}(\phi) \approx (4\nu^2/9\pi)[(\phi - \phi_{HS}^{(a)})/\phi]^2$.

C. Method of solution of Eqs. (2.3) and (2.7)–(2.10) for equilibration

For concreteness, let us consider the case in which the system was initially prepared to be in the *equilibrium* state corresponding to a point $(\phi, T^{*(i)})$ located in the fluidlike region. We then have two fundamentally different possibilities, also illustrated in Fig. 1, either the final point $(\phi, T^{*(f)})$ lies in the ergodic region of the dynamic arrest diagram, or else it lies in the region of dynamically arrested states. The first case is achieved, for example, if the volume fraction of the isochoric irreversible process is smaller than the dynamic arrest volume fraction $\phi^{(a)} = 0.582$ of the hard-sphere liquid. This isochoric quench $(\phi, T^{*(i)}) \to (\phi, T^{*(f)})$ will then eventually lead to the full equilibration of the system. In the second case, in which the fixed volume fraction ϕ must be larger than $\phi^{(a)} = 0.582$ (and the final temperature sufficiently low), the solution of Eqs. (2.3) and (2.7)–(2.10) will describe the irreversible aging of the glass-forming liquid quenched to a point inside the dynamically arrested region.

In either case, solving Eq. (2.3) for $S(k;t)$ starts with the formal solution in Eq. (2.4), written as

$$S^*(k;u) = S^{(i)}(k)e^{-\alpha(k)u} + S_f^{eq}(k)(1 - e^{-\alpha(k)u}). \quad (3.2)$$

This expression interpolates $S^*(k;u)$ between its initial value $S^{(i)}(k) = S^{(eq)}(k;\phi, T^{*(i)})$ and its expected long-time equilibrium value $S_f^{eq}(k) \equiv S^{(eq)}(k;\phi, T^{*(f)}) = [\overline{n}^{(f)}\mathcal{E}^{(f)}(k)]^{-1}$. Clearly, the solution $S(k;t)$ in Eq. (2.4) can be written as

$$S(k;t) = S^*(k;u(t)), \quad (3.3)$$

with $u(t)$ defined in Eq. (2.6). The inverse function $t(u)$ is such that $u(t(u')) = u'$ and $t(u(t')) = t'$. The differential form of Eq. (2.6) can be written as $dt = du(t)/b(t)$. Upon integrating this equation, we have that $t = \int_0^t du(t')/b(t')$, which can also be written, after the change of the integration variable t', to $u' \equiv u(t')$, as

$$t(u) \equiv \int_0^u \frac{1}{b^*(u')} du', \quad (3.4)$$

with the function $b^*(u)$ defined as $b^*(u) = b(t(u))$. These general observations greatly simplify the mathematical analysis and the numerical method of solution of the full NE-SCGLE theory under the particular conditions considered here.

To see this, let us consider a sequence $S^*(k;u_n)$ of snapshots of the static structure factor, generated by the simple expression in Eq. (3.2) when the parameter u attains a sequence of equally spaced values u_n, say $u_n = n\Delta u$ (with a prescribed Δu and with $n = 0,1,2,\ldots$). The fact that $S(k;t)$ can be written as $S(k;t) = S^*(k;u(t))$ implies that this sequence will be identical to the sequence $S(k;t_n)$ generated by the exact solution in Eq. (2.4), evaluated at a different sequence t_n ($n = 0,1,2,\ldots$), i.e., at a sequence of values of the time t, given by $t_n = \int_0^{u_n}[1/b^*(u')]du'$. In other words, the nth member of the sequence of static structure factors can be labeled either with the label u_n, as $S^*(k;u_n)$, or with the label t_n, as $S(k;t_n)$. For sufficiently small Δu, the discretized form of the previous relationship between t_n and u_n can be written as

$$t_{n+1} = t_n + \Delta u/b^*(u_n). \quad (3.5)$$

Thus, in practice what we do is to solve the self-consistent system of Eqs. (2.7)–(2.11) with $S(k;t)$ replaced with each snapshot $S(k;t_n) = S^*(k;u_n)$ of the sequence of static structure factors. This yields, among all the other dynamic properties, the sequence of values $b^*(u_n)$ of the function $b^*(u)$. This sequence can then be used in the recurrence relation in Eq. (3.5) to obtain the desired time sequence t_n, which allows us to ascribe a well-defined time label to the sequence $S(k;t_n)$ of static structure factors and to the sequence $b(t_n)$ of the instantaneous mobility $b(t)$. Of course, since the solution of Eqs. (2.7)–(2.11) yields all the dynamic properties, we also have in store the corresponding sequence of snapshots of dynamic properties such as $F(k,\tau;t_n)$, $F_S(k,\tau;t_n)$, the α-relaxation time $\tau_\alpha(t_n)$, etc.

IV. EQUILIBRATION OF SOFT-SPHERE LIQUIDS

We have applied the protocol just described, which solves the full NE-SCGLE theory [Eqs. (2.4)–(2.11)], to the description of the isochoric irreversible evolution of the structure and the dynamics of the TLJ soft-sphere liquid, after the instantaneous quench starting from an equilibrium fluid state. To continue the analysis, however, it is convenient to discuss separately the two mutually exclusive possibilities illustrated by the two vertical arrows in Fig. 1. In this section we concentrate on the conceptually simplest case of the full equilibration of the system, and in the following section we discus the process of dynamic arrest.

A. Ordered sequence of nonequilibrium static structure factors

Let us thus illustrate the isochoric quench in which both the initial and the final points lie in the fluidlike region. For concreteness, we consider a cooling process, $T^{(i)} > T^{(f)}$, such that $b^{(i)} > b^{(f)} > 0$, with $T^{*(i)} = 0.1$, $\phi = 0.56$ ($<\phi^{(a)} = 0.582$), and with the final temperature corresponding to the deepest quench, $T^{*(f)} = 0$. The initial and final equilibrium static structure factors, $S^{(i)}(k) = S^{(eq)}(k;\phi_1, T^{*(i)})$ and $S_f^{eq}(k) = S^{(eq)}(k;\phi_1, T^{*(f)})$, are presented in Fig. 2. To visualize the transient nonequilibrium relaxation of $S(k;t)$, we generate a sequence of snapshots $S^*(k;u_n)$ using Eq. (3.2) with $u = u_n = n\Delta u$ ($n = 0,1,2,\ldots$) and with

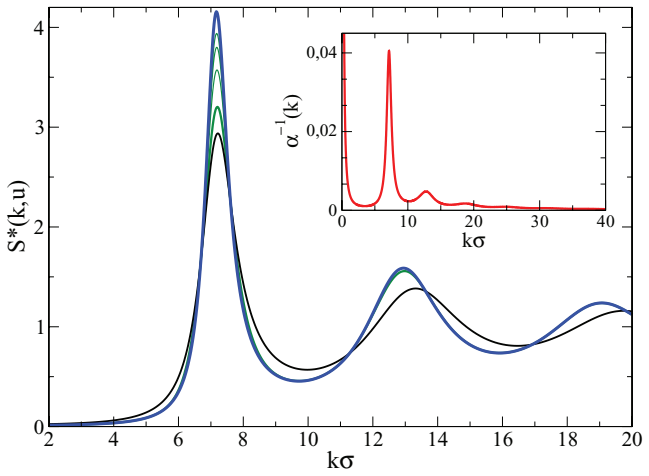

FIG. 2. (Color online) Snapshots of the time-evolving static structure factor $S^*(k;u)$ corresponding to the quench $(\phi, T^{*(i)}) \to (\phi, T^{*(f)})$ at fixed volume fraction $\phi = 0.56$ and $T^{*(i)} = 0.1$ and $T^{*(f)} = 0$. The darker thick (black) solid line is the initial structure factor $S^*(k;u=0) = S^{(i)}(k)$. The lighter thick (blue) solid line is the asymptotic limit $S^*(k;u\to\infty) = S_f^{eq}(k)$. The sequence of thinner (green) solid lines represent $S^*(k;u)$ for $u = \Delta u$, $3\Delta u$, $5\Delta u$, and $7\Delta u$ (from bottom to top), with $\Delta u = 0.01$ (we use $[\sigma^2/D^0]$ as the time unit). These six structure factors also correspond, according to Eq. (3.4), to $S(k;t)$ for $t = 0$, 0.036, 0.1, 0.2, 0.533, and ∞. (Inset) Inverse relaxation constant $\alpha^{-1}(k) = S_f^{eq}(k)/2k^2D^0$.

$\Delta u = 0.01[\sigma^2/D^0]$ [$\approx 1/4\alpha(k)$, for $k = k_{\max}$, the position of the main peak of $S_f^{eq}(k)$]. From now on we use $[\sigma^2/D^0]$ as the time unit and σ as the unit length. In Fig. 2 we include four representative intermediate snapshots of this sequence, corresponding to $u/\Delta u = 1$, 3, 5, and 7. Let us emphasize that although these snapshots of the transient structure factor are linear combinations of two equilibrium static structure factors [namely, $S^{(i)}(k)$ and $S_f^{eq}(k)$], they themselves represent fully nonequilibrium structures.

Figure 2 exhibits the fact that within the resolution $\Delta u = 0.01$ employed to visualize $S^*(k;u)$, this nonequilibrium structure relaxes very quickly to its long-time equilibrium limit $S_f^{eq}(k)$ at most wave vectors, except in two regions: In the vicinity of $k_{\max}$ (corresponding to the ordinary de Gennes narrowing [39]), as appreciated in the figure, and in the long-wavelength limit, $k \to 0$, not apparent in the main figure, but illustrated and discussed below. Thus, except in these two wave-vector domains, the nonequilibrium snapshots of $S^*(k;u)$ shown in the figure are already indistinguishable from $S_f^{eq}(k)$. The fact that for large wave vectors, $k > k_{\max}$, the structure $S^*(k;u)$ approaches very fast its final equilibrium value $S_f^{eq}(k)$ is understood by the fact that $\alpha(k) = 2k^2D^0/S_f^{eq}(k)$ increases with k^2 while $S_f^{eq}(k)$ decreases from its maximum value towards its unit value at large k. To the left of $k_{\max}$, on the other hand, although $\alpha(k)$ decreases with k^2, there is a dramatic drop of the static structure factor from its large value at the main peak towards the very small value of $S_f^{eq}(k=0)$ of a strongly incompressible liquid. In support of this proposed scenario, in the inset of Fig. 2 we plot the inverse relaxation constant $\alpha^{-1}(k) = S_f^{eq}(k)/2k^2D^0$ as a function of k, which clearly exhibits a dominant peak at $k = k_{\max}$, and a divergence at $k = 0$. This explains the quick thermalization of $S^*(k;u)$ in both, the large wave-vector domain and in the moderately small wave-vector regime $0 < k \lesssim k_{\max}$.

In the really small wave-vector limit $k \to 0$, however, the $1/k^2$ divergence of $u_{eq}(k)$ dominates and prevents the thermalization of $S^*(k;u)$ within finite values of u. The crossover from this long-wavelength perfect slowdown to the faster moderately small wave-vector regime $k \lesssim k_{\max}$ is revealed by zooming in at the small-k behavior of the snapshots of $S^*(k;u)$, as illustrated in Fig. 3(a). In contrast with this rather trivial long-wavelength slowing down, the slow relaxation at and around $k = k_{\max}$ has its origin in the large value attained by $S_f^{eq}(k_{\max})$, i.e., in the large strength of the interparticle correlations of spatial extent similar to the mean distance between the particles. Thus, this slowing down of the main peak of the u-evolving static structure factor is a nonequilibrium manifestation of the so-called cage effect. In Fig. 3(b) we present a magnification of the snapshots of $S^*(k;u)$ of Fig. 2, exhibiting in more detail the slower relaxation of the structure at these wave vectors.

B. Nonequilibrium u dependence of $S^*(k;u)$ and $b^*(u)$

Let us notice that the simple expression for $S^*(k;u)$ in Eq. (3.2), which interpolates this function of u between $S^{(i)}(k)$

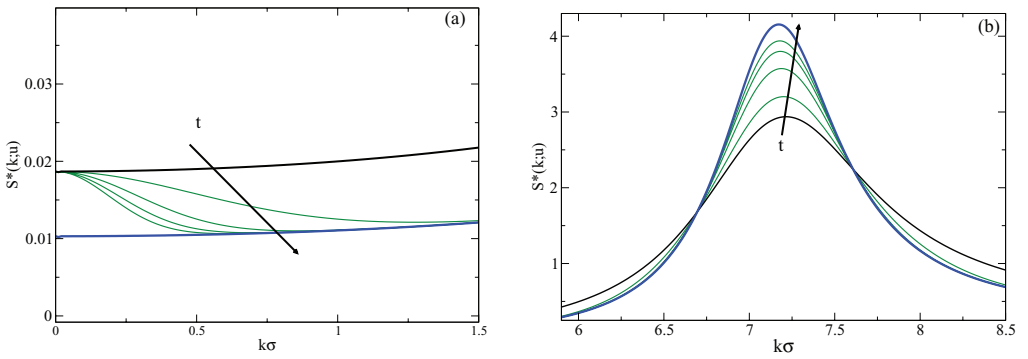

FIG. 3. (Color online) Magnification of the snapshots $S^*(k;u_n)$ in Fig. 2 corresponding to (a) the long-wavelength limit $k \to 0$ and (b) to the neighborhood of the position $k_{\max}$ of the main peak of $S_f^{eq}(k)$.

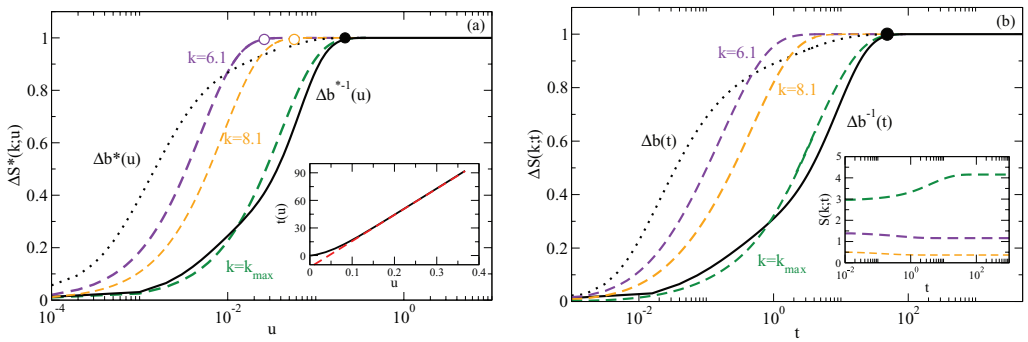

FIG. 4. (Color online) (a) The function $\Delta S^*(k;u) = 1 - \exp[-\alpha(k)u]$ corresponding to three different wave vectors, $k = 6.1, 7.26\ (=k_{\max})$, and 8.1, plotted as a function of the parameter u (dashed lines). The circles correspond to $u = u_{eq}(k) = 5\alpha^{-1}(k)$, where $[1 - \Delta S^*(k;u_{eq}(k))] = e^{-5}$. The dotted and the solid dark lines represent, respectively, the functions $\Delta b^*(u)$ and $\Delta b^{*-1}(u)$ [Eqs. (4.2) and (4.3)], and the solid circle corresponds to the estimated equilibration value $u^{eq} = u_{eq}(k_{\max})$. The inset compares the function $t(u)$ calculated according to its exact definition in Eq. (3.4) (solid line) and according to the approximation in Eq. (4.6). (b) Same information as in (a), but now plotted as a function of the actual *evolution* time $t \equiv \int_0^u \frac{1}{b^*(u')} du'$. In the main figure we plot $\Delta S(k;t)$ and in the inset we plot $S(k;t)$.

and $S_f^{eq}(k)$, may be written as

$$\Delta S^*(k;u) \equiv \frac{S^*(k;u) - S^{(i)}(k)}{S_f^{eq}(k) - S^{(i)}(k)} = 1 - e^{-\alpha(k)u}. \quad (4.1)$$

This means that if we plot the static structure factor $S^*(k;u)$ as $\Delta S^*(k;u)$ vs the k-dependent variable $[\alpha(k)u]$, the results for all the wave vectors k must collapse onto a master curve independent of k and of the initial and final values $S^{(i)}(k)$ and $S_f^{eq}(k)$. In fact, such a master curve will be essentially a simple exponential function. This simplicity, however, will be partially lost if we plot $\Delta S^*(k;u)$ directly as a function of the parameter u, since such exponential function, $e^{-\alpha(k)u}$, will decay with u at a different rate $\alpha(k)$ for different values of the wave vector k, as illustrated in Fig. 4(a). In fact, if we define a k-dependent *equilibration* value $u_{eq}(k)$ by the condition $e^{-\alpha(k)u_{eq}(k)} \approx e^{-5}$, we have that $u_{eq}(k) \equiv 5\alpha^{-1}(k)$. Thus, except for the arbitrary factor of 5, the inset of Fig. 2(a) exhibits the wave-vector dependence of $u_{eq}(k)$. There we see that $u_{eq}(k)$ attains its largest value at the wave vector $k_{\max}$, corresponding to the position of the main peak of $S_f^{eq}(k)$. This slowest mode imposes the pace of the overall equilibration process, thus characterized by the k-independent *equilibration* value $u^{eq} \equiv u_{eq}(k_{\max}) = 5S_f^{eq}(k_{\max})/2k_{\max}^2 D^0$.

The previous discussion illustrates the properties of the ordered sequence $S^*(k;u_n)$ of snapshots of the function $S^*(k;u)$ for equally spaced values u_n of the parameter u. This sequence of snapshots, however, does not fully reveal the most important features of the real relaxation scenario implied by the solution (2.4) of Eq. (2.3), which provides $S(k;t)$ as a function of the actual evolution time t. Nevertheless, since $S(k;t_n) = S^*(k;u(t_n))$, these features are fully revealed by simply relabeling the referred sequence $S^*(k;u_n)$ using the (not equally spaced) sequence of labels t_n given by the recurrence relation in Eq. (3.5). This results in the sequence $S(k;t_n)$ of snapshots that describes the actual time evolution of $S(k;t)$. In order to carry out this program, however, we must first determine the sequence $b^*(u_n)$ needed in the referred recurrence relation.

As indicated before, from any sequence of snapshots $S^*(k;u_n)$, with $u = n\Delta u$ $(n = 0,1,2,\ldots)$, we may generate a sequence $b^*(u_n)$ of values of the time-dependent mobility $b^*(u)$ by solving the self-consistent system of equations (2.7)–(2.11) with $S(k;t)$ replaced with $S^*(k;u_n)$ for each snapshot. The resulting sequence $b^*(u_n)$ is a discrete representation of the function $b^*(u)$, shown in Fig. 4(a), whose resolution in the parameter u may be improved arbitrarily by taking Δu as small as needed. The first feature to notice in the result of this procedure is the fact that $b^*(u)$ decays monotonically from its initial value b_i to its final value $b_f > 0$. This implies that the system will always remain fluidlike and will have no impediment to reach its expected equilibrium state. We also find that the function $b^*(u)$ attains its asymptotic value b_f for $u > u^{eq}$ ($\approx$0.2 for the quench illustrated in the figure).

In Fig. 4(a) we also present the results for $b^*(u)$ plotted as

$$\Delta b^*(u) \equiv \frac{b^*(u) - b_i}{b_f - b_i}. \quad (4.2)$$

We see that this plot does not exhibit any simple relationship between the decay of $\Delta b^*(u)$ and the decay of $\Delta S^*(k;u)$. In the same figure, however, the results for $b^*(u)$ are plotted as

$$\Delta b^{*-1}(u) \equiv \frac{b^{*-1}(u) - b_i^{-1}}{b_f^{-1} - b_i^{-1}}. \quad (4.3)$$

Plotted in this manner we observe a more apparent correlation between the decay of both $\Delta S^*(k_{\max};u)$ and $\Delta b^{*-1}(u)$ with the parameter u. This feature remains, of course, when these properties are expressed as functions of the actual evolution time t, as we now see.

C. Real-time dependence of $S(k;t)$ and $b(t)$

Once we have determined the function $b^*(u)$, using the expression for $t(u)$ in Eq. (3.4), or its discretized version in the recursion relation of Eq. (3.5), we can determine the desired real-time evolution of $S(k;t)$ and $b(t)$. In this manner we determine that in our illustrative example the sequence $u = 0$, 0.01, 0.03, 0.05, and 0.07 corresponds to the sequence

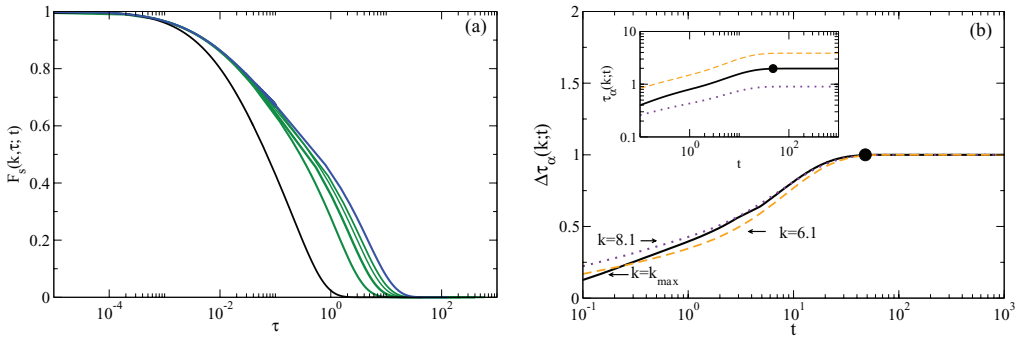

FIG. 5. (Color online) (a) Snapshots of the nonequilibrium self intermediate scattering function $F_S(k,\tau;t)$ at $k = k_{\max}$, corresponding to the equilibration process in Fig. 2 for evolution times $t = 0$, 0.036, 0.1, 0.2, 0.533, and ∞. (b) Nonequilibrium evolution of the dimensionless α-relaxation time, displayed as $\tau_\alpha(k;t)$ itself (inset) and formatted as in Eq. (4.8) (main figure). The solid circle represents the equilibration point $[t^{eq},\tau_\alpha(k_{\max};t^{eq})]$.

$t = 0$, 0.036, 0.1, 0.2, and 0.533. In the inset of Fig. 4(b) we present the resulting time-evolution of $S(k;t)$ for the same three wave vectors as in Fig. 4(a). This inset emphasizes the fact that $S(k;t)$ evolves monotonically from its initial value $S^{(i)}(k)$ to its final value $S_f^{eq}(k)$, sometimes increasing and sometimes decreasing, depending on the wave vector considered. In order to exhibit a less detail-dependent scenario, in the main frame of Fig. 4(b) we present the same information, but formatted as $\Delta S(k;t)$, which is the relabeled version $(u \to t = t(u))$ of $\Delta S^*(k;u)$ in Eq. (4.1), namely, as

$$\Delta S(k;t) \equiv \frac{S(k;t) - S^{(i)}(k)}{S_f^{eq}(k) - S^{(i)}(k)}. \tag{4.4}$$

We similarly relabel the definitions of $\Delta b^*(u)$ and $\Delta b^{*-1}(u)$ in Eqs. (4.2) and (4.3) to define the functions $\Delta b(t)$ and $\Delta b^{-1}(t)$, which are also plotted in Fig. 4(b). The comparison of this figure with Fig. 4(a) indicates that, except for the stretched metric of t, the overall scenario described by the u dependence illustrated in Fig. 4(a) is preserved in the t dependence illustrated in Fig. 4(b).

Let us notice in particular that the existence of the equilibration value u^{eq} of the parameter u, beyond which $b^*(u) \approx b_f$, allows us to define an *equilibration* time, t^{eq}, as the time that corresponds to u^{eq} through Eq. (3.4),

$$t^{eq} \equiv \int_0^{u^{eq}} \frac{du'}{b^*(u')}. \tag{4.5}$$

For our specific illustrative example, this yields $t^{eq} \approx 48$. The fact that $b^*(u) \approx b_f$ for $u \gtrsim u^{eq}$ implies, according to Eq. (3.4), that for $u > u^{eq}$ the function $t(u)$ will be linear in u, i.e.,

$$t(u) \approx -a(u^{eq}) + b_f^{-1}u, \tag{4.6}$$

with $a(u^{eq}) \equiv \int_0^{u^{eq}} [1/b_f - 1/b^*(u')]du'$. In the inset of Fig. 4(a) we compare this asymptotic expression, applied to our illustrative case [for which $b_f^{-1} = 285$ and $a(u^{eq}) = 12.8$], with the actual $t(u)$ calculated from Eq. (3.4).

D. Irreversibly evolving dynamics

Since for each snapshot of the static structure factor $S(k;t)$ the solution of Eqs. (2.7)–(2.11) determines a snapshot of each of the dynamic properties of the system, the process of equilibration may also be observed, for example, in the t evolution of the collective and self-intermediate scattering functions, $F(k,\tau;t)$ and $F_S(k,\tau;t)$. In Fig. 5(a) we illustrate this irreversible time evolution with the snapshots of the self-ISF $F_S(k_{\max},\tau;t)$, corresponding to the same set of evolution times t_n as the snapshots of $S(k;t)$ in Fig. 2. We see that the function $F_S(k,\tau;t)$ starts from its initial value $F_S(k,\tau;t=0) = F_S^{eq}(k,\tau;\phi,T_i = 0.1)$ and quickly evolves with waiting time t towards the vicinity of its final equilibrium value $F_S(k,\tau;t=\infty) = F_S^{eq}(k,\tau;\phi,T_f = 0)$.

The equilibration process of $F_S(k,\tau_\alpha;t)$ can be best summarized in terms of the dependence of the α-relaxation time $\tau_\alpha(k;t)$ as a function of the evolution time t. The α-relaxation time may be defined by the condition

$$F_S(k,\tau_\alpha;t) = 1/e. \tag{4.7}$$

The dependence of $\tau_\alpha(k;t)$ on the evolution time t can be extracted from a sequence of snapshots of $F_S(k,\tau_\alpha;t)$, such as those in Fig. 5(a). The results are illustrated in Fig. 5(b), in which the solid line corresponds to $\tau_\alpha(k_{\max};t)$. The solid circle indicates the crossover from the t regime where $\tau_\alpha(k_{\max};t)$ is still in the process of equilibration, to the regime where it has reached its final equilibrium value $\tau_\alpha^{(f)}(k_{\max}) \equiv \tau_\alpha^{eq}(k_{\max};\phi,T_f)$. In the inset of the figure we plot $\tau_\alpha(k_{\max};t)$ itself and in the main figure we plot the same information, but formatted as

$$\Delta\tau_\alpha(k;t) \equiv \frac{\tau_\alpha(k;t) - \tau_\alpha^{(i)}(k)}{\tau_\alpha^{(f)}(k) - \tau_\alpha^{(i)}(k)}, \tag{4.8}$$

with $\tau_\alpha^{(i)}(k) \equiv \tau_\alpha^{eq}(k;\phi,T_i)$. In the same figure we also exhibit similar results corresponding to two additional wave vectors, different from $k_{\max}$ (dashed lines). These results show that the equilibration time of $\tau_\alpha(k;t)$ for these three wave vectors is largely independent of k, and can be well approximated by the equilibration time t^{eq} defined in Eq. (4.5), in contrast with the notorious wave-vector dependence of the predicted evolution of the static structure factor illustrated in Fig. 4(b).

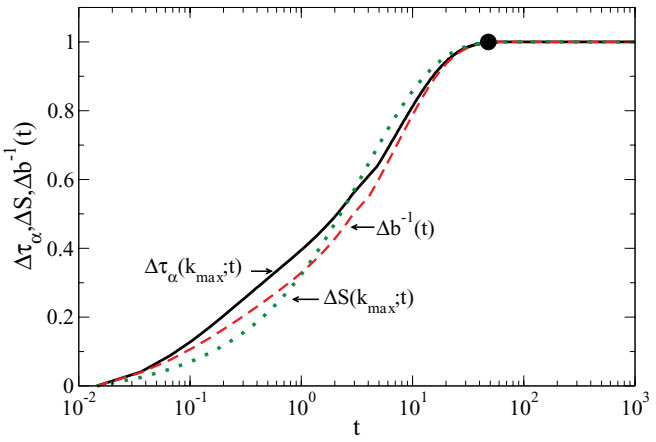

FIG. 6. (Color online) Time-evolving α-relaxation time $\tau_\alpha(k_{\max};t)$ (solid line), mobility $b(t)$ (dashed line), and static structure factor $S(k_{\max};t)$ (dotted line) as a function of evolution time t and expressed as $\Delta\tau_\alpha(k_{\max};t)$, $\Delta b^{-1}(t)$, and $\Delta S(k_{\max};t)$.

Let us finally mention another theoretical prediction regarding the kinetics of the equilibration process. This refers to the similarity of the equilibration kinetics exhibited by the time-dependent mobility $b(t)$, the α-relaxation time $\tau_\alpha(k;t)$ at all wave vectors, and the static structure factor $S(k_{\max};t)$ at the wave vector $k_{\max}$, when plotted in terms of the reduced properties $\Delta b(t)^{-1}$, $\Delta\tau_\alpha(k;t)$, and $\Delta S(k_{\max};t)$. This similarity is exhibited in Fig. 6 for the illustrative quench at fixed $\phi = 0.56$, and means that indeed the evolution of $S(k_{\max};t)$ [which is slower than the evolution of $S(k;t)$ for other wave vectors] sets the overall relaxation rate exhibited by the dynamic properties $\Delta b(t)^{-1}$ and $\Delta\tau_\alpha(k;t)$. Thus, from this point of view, we may use either of these characteristic dynamic properties to describe the predicted kinetics of the equilibration process.

E. Dependence on the initial temperature of the quench

Up to this point we have illustrated the main features of the isochoric quench $(\phi, T^{*(i)}) \to (\phi, T^{*(f)})$ at fixed volume fraction $\phi = 0.56$, using for concreteness the values $T^{*(i)} = 0.1$ and $T^{*(f)} = 0$. We are now ready to analyze how the scenario just described depends on the initial temperature $T^{*(i)}$ and on the volume fraction ϕ at which we perform the quench. Let us start by considering the dependence on $T^{*(i)}$. Rather than attempting a comprehensive illustration of this dependence in terms of the evolution of the static structure factor $S(k;t)$ and of the various dynamic properties, we use the dimensionless mobility $b(t)$ as a representative property bearing the essential information about the equilibration process. This k-independent property determines the mapping from the parameter u to the real time t, through the definition of the functions $u(t)$ and $t(u)$ in Eqs. (2.6) and (3.4).

Thus, in Fig. 7(a) we present plots of $b^{-1}(t)$ as a function of t for three representative values of the initial temperature $T^{*(i)}$, namely, $T^{*(i)} = 1.0$, 0.1, and 0.01, keeping the same final temperature $T^{*(f)} = 0$ and the same volume fraction $\phi = 0.56$. This figure reveals two remarkable features. In the first place, the equilibration time t^{eq} seems to be rather insensitive to the temperature $T^{*(i)}$ of the initial state. In other words, the system will reach the final equilibrium state in about the same time, $t^{eq} \approx 48$, no matter if the initial temperature is $T^{*(i)} = 1.0$, 0.1, or 0.01. To emphasize this feature we have highlighted the common equilibration point of the three curves. The second remarkable feature is that during the transient stage of the equilibration process, the evolution of $b^{-1}(t)$ as a function of t follows approximately a power law, $b^{-1}(t) \approx At^x$, with the exponent x and the amplitude A depending on the initial temperature $T^{*(i)}$. In the inset of the figure we exhibit the power law fit of the transient, indicating the resulting value of the exponent x and amplitude A.

Exactly the same trend is also reflected in the evolution of the intermediate scattering function, as observed in the results for the α-relaxation time shown in Fig. 7(b). This information is important, since many times it is this dynamic parameter that is monitored in simulations and in some experiments.

F. Dependence on the volume fraction of the quench

Let us now discuss the dependence of the equilibration process on the volume fraction ϕ. Once again we first use the time evolution of $b(t)$ to illustrate this dependence. In Fig. 8(a) we plot $b^{-1}(t)$ as a function of t for a set of values of the volume fraction ϕ, corresponding to the metastable regime of

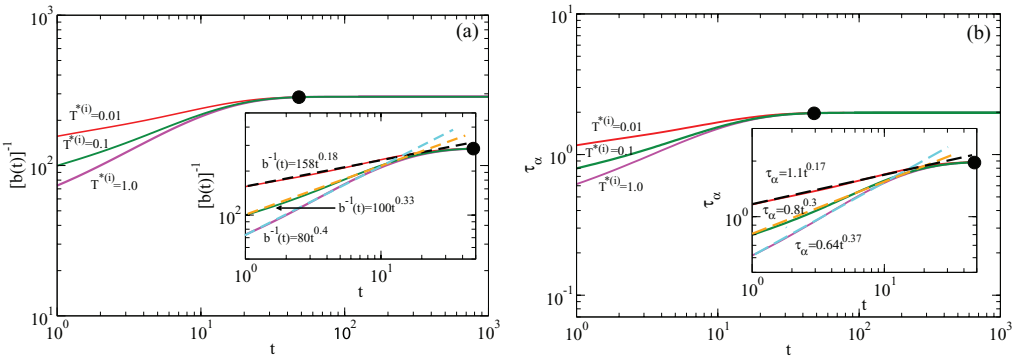

FIG. 7. (Color online) Nonequilibrium, time-dependent (a) mobility $b(t)$ and (b) α-relaxation time $\tau_\alpha(t)$, as a function of evolution time t, for the isochoric quench $(\phi, T^{*(i)}) \to (\phi, T^{*(f)} = 0)$ at fixed volume fraction $\phi = 0.56$, for three different initial temperatures, $T^{*(i)}$= 1.0, 0.1, and 0.01. The insets exhibit a power law fit of the transient before saturation.

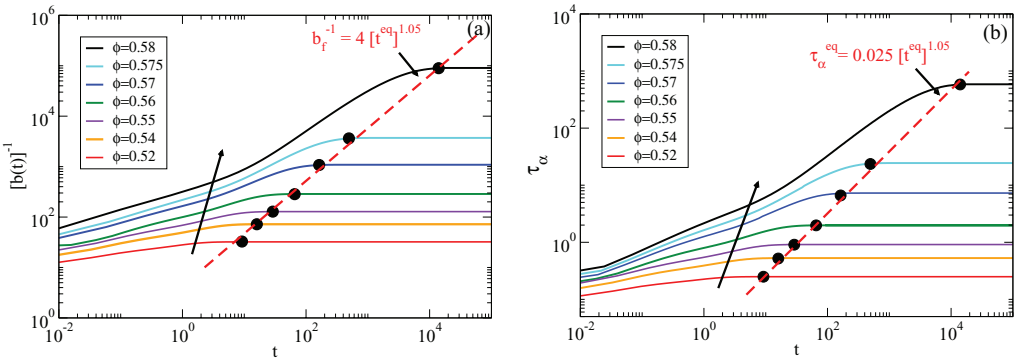

FIG. 8. (Color online) Nonequilibrium, time-dependent (a) mobility $b^{-1}(t)$ and (b) α-relaxation time $\tau_\alpha(t)$ as a function of evolution time t for various volume fractions corresponding to the metastable regime of the hard-sphere liquid. The arrows indicate the direction of increasing ϕ. The dashed lines are the power laws $b_f^{-1}(\phi) \approx 4 \times [t^{eq}(\phi)]^{1.05}$ and $\tau_\alpha^{eq}(\phi) \approx 0.025 \times [t^{eq}(\phi)]^{1.05}$.

the hard-sphere liquid. According to these results, the inverse mobility $b^{-1}(t;\phi)$ reaches its equilibrium value $b_f^{-1}(\phi)$ after a ϕ-dependent equilibration time $t^{eq}(\phi)$. To emphasize this prediction, the solid circles in the figure highlight the points $(t^{eq}(\phi), b_f^{-1}(\phi))$. These highlighted points, as indicated in the figure, align themselves to a good approximation along the dashed line of the figure, corresponding to the approximate relationship $b_f^{-1}(\phi) \approx 4 \times [t^{eq}(\phi)]^{1.05}$.

This relationship between the equilibration time $t^{eq}(\phi)$ and $b_f(\phi)$ is one of the most remarkable predictions of the present theory, bearing profound physical implications. To see this, let us recall that the dimensionless mobility $b_f(\phi)$ is just the scaled long-time self-diffusion coefficient $D^*(\phi,T_f) \equiv D_L(\phi,T_f)/D^0$ of the fully equilibrated system at the final point (ϕ,T_f), which for the present isochoric quench down to zero temperature, $T_f = 0$, is the dimensionless equilibrium long-time self-diffusion coefficient of the hard-sphere liquid, $D_{HS}^*(\phi) \equiv D^*(\phi,T_f = 0)$. This property can be calculated using the equilibrium version of the present theory [22] and, as discussed below [see Fig. 9(b)], such calculation leads to the prediction that $D_{HS}^*(\phi)$ vanishes at $\phi^{(a)} = 0.582$, according to the power law $D_{HS}^*(\phi) \propto (\phi^{(a)} - \phi)^{2.2}$. As a consequence, if $t^{eq}(\phi) \approx 0.25 \times b_f^{-1}(\phi)$ $[\propto D_{HS}^{*-1}(\phi)]$, we must expect that as $\phi \to \phi^{(a)}$ the equilibration time will diverge according to $t^{eq}(\phi) \propto (\phi^{(a)} - \phi)^{-2.2}$.

This predicted divergence of the equilibration time constitutes a strong and interesting proposal, which requires, of course, a critical assessment and validation. We return to this discussion later in the paper, but at this point, let us carry out a similar analysis, now using the α-relaxation time $\tau_\alpha(t;\phi)$ (whenever we omit the wave vector k as the argument of $\tau_\alpha(k,t;\phi)$ it is because a specific value for k is being assumed fixed, most frequently $k \approx k_{\max}$). Thus, in Fig. 8(b) we plot $\tau_\alpha(t;\phi)$ as a function of t for the same set of values of the volume fraction ϕ as in Fig. 8(a). Here again we find that $\tau_\alpha(t;\phi)$ reaches its equilibrium value $\tau_\alpha^{eq}(\phi)$ after the same evolution time $t^{eq}(\phi)$ as in the case of $b(t;\phi)$. Also here the solid circles highlight the points $(t^{eq}(\phi), \tau_\alpha^{eq}(\phi))$, and the dashed line in the figure implies that $t^{eq}(\phi) \approx 40 \times [\tau_\alpha^{eq}]^{0.95}(\phi)$. This implies that the time $t^{eq}(\phi)$ required to equilibrate the system will grow at least about as fast as the equilibrium value τ_α^{eq} of the α-relaxation time and that both properties increase strongly with ϕ.

Although one can discuss additional features of the class of irreversible process corresponding to the full isochoric equilibration of the system after its sudden cooling, it is now important to contrast the scenario just described with that of the second class of irreversible processes. This involves the dynamic arrest of the system and is the subject of the following section.

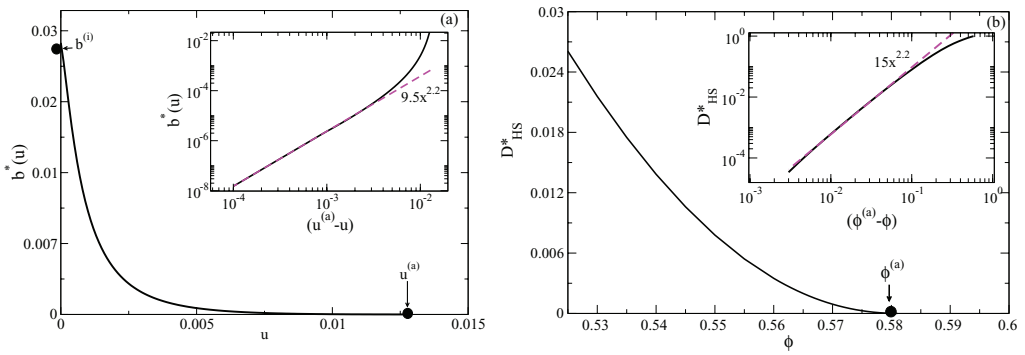

FIG. 9. (Color online) (a) Mobility function $b^*(u)$ plotted as a function of the parameter u and of the difference $(u^{(a)} - u)$ (inset) for the sudden isochoric cooling from the point $(\phi = 0.6, T^{*(i)} = 0.1)$ to the point $(\phi = 0.6, T^{*(f)} = 0)$. (b) Scaled long-time self-diffusion coefficient $D_{HS}^*(\phi) \equiv D_L(\phi)/D^0$ of the hard-sphere liquid as a function of volume fraction ϕ and of the difference $(\phi^{(a)} - \phi)$ (inset).

V. AGING OF SOFT-SPHERE LIQUIDS

Let us recall at this point that the NE-SCGLE description of the spontaneous evolution of the structure and dynamics of an *instantaneously* and *homogeneously* quenched liquid is provided by the simultaneous solution of Eqs. (2.3)–(2.10). As discussed in Sec. III B, there exist two fundamentally different classes of irreversible isochoric processes, represented by the vertical downward arrows in Fig. 1. In the previous section we described the resulting scenario for the most familiar of them, namely, the full isochoric equilibration of the system. In this section we present the NE-SCGLE description of the second class of irreversible isochoric processes, in which the system starts in an ergodic state and ends in the region where it is expected to become dynamically arrested.

Thus, let us continue considering the TLJ model system introduced in Sec. III [Eq. (3.1), with $\nu = 6$], subjected to the sudden isochoric cooling at fixed volume fraction $\phi = 0.6$, larger than $\phi^{(a)} = 0.582$, from the point $(\phi, T^{*(i)} = 0.1)$ in the ergodic region, to the point $(\phi, T^{*(f)} = 0)$ in the region of dynamically arrested states. By construction, the solution $\gamma^{(i)}$ of Eq. (2.14), obtained using $S^{(eq)}(k;\phi,T^{*(i)})$ as the structural input, is $\gamma^{(i)} = \infty$. In this sense, the present class of process is identical to the first one, discussed in the previous section. The main difference lies, of course, in the fact that in the present case the solution of Eq. (2.14) for the squared localization length $\gamma^{(f)}$, obtained using the equilibrium static structure factor $S^{(eq)}(k;\phi,T^{*(f)})$ of the final point as input, will now have a *finite* value.

To see the consequences of this difference, let us go back to Sec. III C and consider the function $S^*(k;u)$ in Eq. (3.2), with $0 \leqslant u \leqslant \infty$. For each value of u we may use $S^*(k;u)$ in the bifurcation equation (2.14) for $\gamma(t)$, now denoted as $\gamma^*(u)$. Throughout the previous section it was implicitly assumed that $\gamma^*(u) = \infty$ for $0 \leqslant u \leqslant \infty$, an assumption based on the fact that the system started and ended in a fluidlike state. In the present case, however, although the system starts with the condition that $\gamma^*(u = 0) = \infty$, we know that the final point $(\phi, T^{*(f)} = 0)$ corresponds to an arrested state, so that $\gamma^{(f)} \equiv \gamma^*(u = \infty)$ has a finite value. This means that somewhere between $u = 0$ and $u = \infty$ the function $\gamma^*(u)$ changed from infinity to a finite value, and this then implies the existence of a finite value $u^{(a)}$ of u, such that $\gamma^*(u)$ remains infinite only within the interval $0 \leqslant u < u^{(a)}$. Thus, in the present case the simultaneous solution of Eqs. (2.3)–(2.10) starts in practice with the precise determination of $u^{(a)}$.

A. Method of solution of Eqs. (2.3) and (2.7)–(2.10) for aging

To determine the critical value $u^{(a)}$, let us consider again the sequence $S^*(k;u_n)$ of snapshots of the static structure factor, generated by the expression in Eq. (3.2) with $u_n = n\Delta u$ ($n = 0,1,2,\ldots$). Since we have assumed that initially the system is fluidlike, the value of $u^{(a)}$ cannot be $u^{(a)} = 0$. Thus, let us employ each snapshot of the sequence $S^*(k;u_n)$, with $n = 1,2,\ldots$, as the static input of Eq. (2.14), thus determining the sequence $\gamma_n^* \equiv \gamma^*(u_n)$ of values of $\gamma^*(u)$, which starts with $\gamma_0^* = \infty$. If γ_1^* turns out to be finite, then one may take a smaller u step Δu, until this does not happen. For a sufficiently small Δu, there will be an integer n_a such that $\gamma_n^* = \infty$ for $n < n_a$ and γ_n^* is finite for $n > n_a$, i.e., such that $u_{n_a} < u^{(a)} < u_{(n_a+1)}$. This process can be refined by decreasing Δu, so that one can determine $u^{(a)}$ with arbitrary precision for the given initial and final conditions $(\phi, T^{*(i)})$ and $(\phi, T^{*(f)})$. For example, one can readily perform this procedure for the quench indicated by the right arrow of Fig. 1 [from the point $(\phi, T^{*(i)} = 0.1)$ to the final point $(\phi, T^{*(f)} = 0)$ at fixed $\phi = 0.6$], with the result $u^{(a)} = 0.0128$.

Once one has determined $u^{(a)}$ with the desired precision, one can construct a new sequence u_l of $(N+1)$ equally spaced values of u, defined as $u_l \equiv l \times (u^{(a)}/N)$ with $0 \leqslant l \leqslant N$, along with the corresponding sequence $S^*(k;u_l)$ of snapshots of the static structure factor [using Eq. (3.2)]. Since the sequence $S^*(k;u_l)$ is identical to the sequence $S(k;t_l)$ [with t_l such that $u_l = \int_0^{t_l} b(t')dt'$], to each member of this sequence, the self-consistent Eqs. (2.8)–(2.10) assigns a snapshot of the full dynamics of the system. In particular, the use of Eq. (2.7) generates a sequence of values $b^*(u_l)$ of the mobility $b^*(u)$, with arbitrary resolution (set by the number N of u steps). To illustrate these concepts, in Fig. 9(a) we present the results for $b^*(u)$ corresponding to the specific quench under discussion. Notice that, as expected, $b^*(u) \to 0$ as u approaches $u^{(a)}$ from below.

A simple ansatz to model this limiting behavior is

$$b^*(u) \approx B_0(u^{(a)} - u)^{\mu}. \tag{5.1}$$

In the inset of Fig. 9(a) we plot $b^*(u)$ vs $(u^{(a)} - u)$ to determine the value of the exponent μ and the prefactor B_0, with the result $\mu = 2.2$ and $B_0 = 9.5$. We performed similar calculations varying the initial temperature $T^{*(i)}$, and found the value $\mu = 2.2$ of the exponent is independent of $T^{*(i)}$, so that the dependence of $b^*(u)$ on the initial temperature is carried only in the prefactor B_0. For example, we found that $B_0(T^{*(i)}) = 9.5$, 33, and 490, for $T^{*(i)} = 0.1$, 0.05, and 0.01, respectively.

Another remarkable feature of the u dependence of $b^*(u)$ illustrated in the inset of Fig. 9(a) is its similarity with the volume fraction dependence of the scaled long-time self-diffusion coefficient of the *fully equilibrated* hard-sphere system, $D_{HS}^*(\phi) \equiv D_L(\phi, T_f = 0)/D^0$. This property can be calculated using the equilibrium version of the SCGLE theory [22], and the results are exhibited in Fig. 9(b). As discussed before [23], the theoretical prediction is that $D_{HS}^*(\phi)$ vanishes at the dynamic arrest volume fraction $\phi^{(a)} = 0.582$. The results of Fig. 9(b) show that in the vicinity of $\phi^{(a)}$, the function $D_{HS}^*(\phi)$ follows the power law $D_{HS}^*(\phi) \propto (\phi^{(a)} - \phi)^{2.2}$; i.e., it vanishes at $\phi^{(a)}$ with the same exponent as $b^*(u)$ vanishes at $u = u^{(a)}$.

1. Asymptotic decay $b(t) \propto t^{-\eta}$

At this point let us notice that the sequence $b^*(u_l)$ must be identical to the sequence $b(t_l)$ of values of $b(t)$ at the times $t_l \equiv \int_0^{u_l} [1/b^*(u')]du'$. The sequence of times t_l can be determined by means of the approximate recurrence relationship in Eq. (3.5), i.e.,

$$t_{l+1} = t_l + \Delta u / b^*(u_l),$$

with $\Delta u \equiv u^{(a)}/N$, and it allows us to transform the sequence $b^*(u_l)$ into the discrete representation $b(t_l)$ of the function

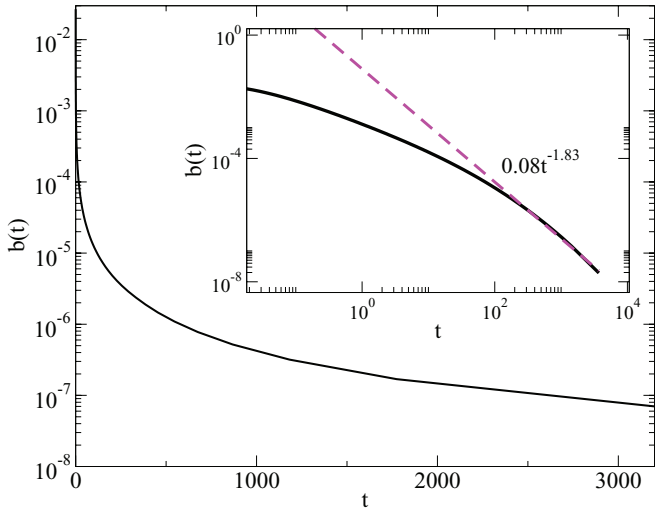

FIG. 10. (Color online) Nonequilibrium mobility $b(t)$ as a function of evolution time t for the quench processes from the point $(\phi = 0.6, T^{*(i)} = 0.1)$ to the point $(\phi = 0.6, T^{*(f)} = 0)$. The inset exhibits the long-t asymptotic decay $b(t) \approx b_0 t^{-\eta}$ described by Eq. (5.6).

$b(t)$. The results for $b(t)$ are plotted in Fig. 10 to exhibit the fundamentally different behavior of the functions $b^*(u)$ and $b(t)$. While the former has a well-defined zero at a finite value of its argument, namely, at $u = u^{(a)}$, the function $b(t)$ decays to zero in a much slower fashion. In fact, as we now discuss, one of the main predictions of the NE-SCGLE theory is that $b(t)$ will remain finite for any finite time t, and only at $t = \infty$ the mobility will reach its asymptotic value of zero. Thus, the system, in principle, will always remain fluidlike, and the dynamic arrest condition $b(t) = 0$ will only be reached after an infinite waiting time.

Let us actually demonstrate that the value of t corresponding to $u^{(a)}$ is $t^{(a)} = \infty$, and that the mobility $b(t)$ decays as a power law with t. To discuss the first issue, let us recall Eq. (3.4), which writes the function $u(t)$ as

$$t(u) = \int_0^u \frac{du'}{b^*(u')}, \tag{5.2}$$

where the function $b^*(u)$ is, of course, $b^*(u) = b(t(u))$. According to this result, and to Eq. (5.1), we can write

$$\begin{aligned} t(u) - t(u_0) &= \int_{u_0}^{u} du'/B_0(u^{(a)} - u')^{\mu} \\ &= \frac{(u^{(a)} - u)^{-(\mu-1)}}{(\mu-1)B_0} - \frac{(u^{(a)} - u_0)^{-(\mu-1)}}{(\mu-1)B_0} \end{aligned} \tag{5.3}$$

for u in some vicinity $u_0 \leqslant u \leqslant u^{(a)}$ of $u^{(a)}$. This implies that, if the exponent μ is larger than unity, then $t(u)$ will diverge as u approaches $u^{(a)}$ according to

$$t(u) \approx \frac{(u^{(a)} - u)^{-(\mu-1)}}{(\mu-1)B_0}. \tag{5.4}$$

As a consequence, the dynamic arrest time $t^{(a)} \equiv t(u^{(a)})$ will be infinite, which is what we set out to demonstrate.

Let us now discuss the possibility that $b(t)$ decays as a power law with t. For this, let us invert the function $t(u)$ in the previous equation and write it as

$$u(t) \approx u^{(a)} - \{(\mu-1)B_0 t\}^{-\frac{1}{(\mu-1)}}. \tag{5.5}$$

Since, according to Eq. (2.6), $b(t) = du(t)/dt$, the time derivative of this asymptotic expression will yield the asymptotic form for $b(t)$, namely,

$$b(t) \approx b_0 t^{-\eta}, \tag{5.6}$$

with

$$b_0 \equiv [(\mu-1)^{\mu} B_0]^{-\frac{1}{(\mu-1)}}, \tag{5.7}$$

and

$$\eta \equiv \frac{\mu}{(\mu-1)} \quad \left(\text{or} \quad (\eta - 1) = \frac{1}{(\mu-1)}\right). \tag{5.8}$$

The latter result implies that if one of the exponents (μ or η) is larger than unity, then the other is also larger than unity. It also implies that if one of them is larger than 2, then the other is smaller than 2, and vice versa. In the inset of Fig. 10 we compare the actual NE-SCGLE results for $b(t)$ in the main figure, with the approximate asymptotic expression in Eq. (5.6) with a fitted exponent η, with the result that $\eta = 1.83$. This value coincides with the expected result $\eta = \mu/(\mu-1)$ with $\mu = 2.2$. As indicated above, we performed similar calculations varying the initial temperature $T^{*(i)}$, and found that the scenario just described is indeed independent of $T^{*(i)}$. Thus, in the asymptotic expression in Eq. (5.6) only the prefactor b_0 depends on $T^{*(i)}$, and the approximate expression in Eq. (5.7) provides an indicative estimate of its actual value.

2. *Dynamically arrested evolution of $S(k;t)$*

The properties of the nonequilibrium mobility function $b(t)$ that we have just described reveals the main feature of the time evolution of the static structure factor $S(k;t)$ when the system is driven to a point (ϕ, T^*) in the region of dynamically arrested states. We refer to the fact that under such conditions, the long-time asymptotic limit of $S(k;t)$ will no longer be the expected equilibrium static structure factor $S^{(eq)}(k;\phi,T^*)$, but another, well-defined nonequilibrium static structure factor $S^{(a)}(k)$, given by

$$S^{(a)}(k) = S^{(i)}(k) e^{-\alpha(k)u^{(a)}} + S_f^{eq}(k)\left(1 - e^{-\alpha(k)u^{(a)}}\right). \tag{5.9}$$

This nonequilibrium static structure factor not only depends on the final point (ϕ, T^*), but also on the protocol of the quench (in the present instantaneous isochoric quench, this means on the initial temperature $T^{*(i)}$).

To see the emergence of this scenario, let us consider the sequence $S^*(k;u_l)$ of snapshots of the static structure factor generated with Eq. (3.2), for the finite sequence u_l of $(N+1)$ equally spaced values of u defined as $u_l \equiv l \times (u^{(a)}/N)$ with $0 \leqslant l \leqslant N$. According to Eq. (5.2), and to its asymptotic version in Eq. (5.4), in the present case the finite range $0 \leqslant u \leqslant u^{(a)}$ maps onto the infinite physically relevant range $0 \leqslant t \leqslant \infty$ of the evolution time t (in contrast with the equilibration processes studied in the previous section, in which the infinite range $0 \leqslant u \leqslant \infty$ maps onto the infinite range $0 \leqslant t \leqslant \infty$). Since the sequence $S^*(k;u_l)$ is identical to the sequence $S(k;t_l)$, with $t_l = \int_0^{u_l} du'/b^*(u')$, then the sequence

of snapshots $S(k;t_l)$ describing the full evolution of $S(k;t)$ will be generated by a sequence of snapshots of $S^*(k;u)$ with u only in the range $0 \leqslant u \leqslant u^{(a)}$. In other words, in the present case none of the snapshots of $S^*(k;u)$ with $u \geqslant u^{(a)}$ will map onto any physically observable snapshot of $S(k;t)$, and this applies in particular to the snapshot $S^*(k;u=\infty)$, corresponding to the expected equilibrium static structure factor $S^{(eq)}(k)$. In this manner, the long time limit of $S(k;t)$, normally being the ordinary equilibrium value $S^{(eq)}(k)$ $(\equiv[\overline{n}\mathcal{E}^{(f)}(k)]^{-1})$, is now replaced by a nonequilibrium dynamically arrested static structure factor $S^{(a)}(k)$ given, according to Eq. (3.2), by the expression in Eq. (5.9).

Besides the remarkable prediction of the existence of this well-defined nonequilibrium asymptotic limit of $S(k;t)$, the second relevant feature refers to the kinetics of $S(k;t)$ as it approaches $S^{(a)}(k)$. To exhibit this feature, let us subtract Eq. (5.9) from Eq. (2.4). This leads to

$$S(k;t) - S^{(a)}(k) = A(k)[e^{-\alpha(k)[u(t)-u^{(a)}]} - 1], \qquad (5.10)$$

with

$$A(k) \equiv e^{-\alpha(k)u^{(a)}}\left\{S^{(i)}(k) - S_f^{eq}(k)\right\}. \qquad (5.11)$$

At long times, when $[u(t) - u^{(a)}]$ is small, this equation reads

$$S(k;t) - S^{(a)}(k) \approx A(k)\alpha(k)[u^{(a)} - u(t)]. \qquad (5.12)$$

From Eq. (5.5), however, we have that $u^{(a)} - u(t) \approx \{(\mu-1)B_0 t\}^{-\frac{1}{(\mu-1)}}$, so that the previous long-time expression for $S(k;t)$ can be written as

$$S(k;t) - S^{(a)}(k) \approx D(k)t^{-\frac{1}{(\mu-1)}}, \qquad (5.13)$$

with

$$D(k) \equiv A(k)\alpha(k)\{(\mu-1)B_0\}^{-\frac{1}{(\mu-1)}}. \qquad (5.14)$$

Thus, we conclude that, contrary to the kinetics of the equilibration process, in which $S(k;t)$ approaches $S^{(eq)}(k)$ in an exponential-like fashion, this time the decay of $S(k;t)$ to its stationary value $S^{(a)}(k)$ follows a power law. At very short times, however, $b(t) \approx b^{(i)}$, and hence, $u(t) \approx b^{(i)}t$. Thus, according to Eqs. (2.4) and (2.6), we have that the very initial evolution of $S(k;t)$ might seem to approach its expected equilibrium value $S^{(eq)}(k) = [\overline{n}\mathcal{E}^{(f)}(k)]^{-1}$ in an apparently "exponential" manner, with a relaxation time $t^{\text{app}} \approx 1/\alpha(k)b^{(i)}$. This apparent initial exponential evolution, however, crosses over very soon to the much slower long-time evolution of $S(k;t)$ described by the asymptotic expression in Eq. (5.13).

Figure 11 illustrates with a sequence of snapshots the predicted nonequilibrium evolution of $S(k;t)$ after the isochoric quench at $\phi = 0.6$ from $T^{*(i)} = 0.1$ to $T^{*(f)} = 0$. There we highlight the initial static structure factor $S^{(i)}(k) = S^{(eq)}(k;\phi,T^{*(i)})$ and the dynamically arrested long-time asymptotic limit $S^{(a)}(k)$ of the nonequilibrium evolution of $S(k;t)$. For reference, we also plot the expected, but inaccessible, equilibrium static structure factor $S^{(eq)}(k;\phi,T^{*(f)}) = 1/\overline{n}\mathcal{E}(k;\phi,T^{*(f)})$ corresponding to the final temperature $T^{*(f)} = 0$. Regarding the kinetics of the nonequilibrium evolution, in the inset we plot the evolution of the maximum of $S(k;t)$ as a function of t to illustrate the fact that $S(k;t)$ approaches $S^{(a)}(k)$ much more slowly, in fact, as the power law $[S^{(a)}(k) - S(k;t)] \propto t^{-0.83}$. For reference, we also plot the maximum of the function $[S^{(i)}(k)e^{-\alpha(k)b^{(i)}t} + [\overline{n}\mathcal{E}^{(f)}(k)]^{-1}(1 - e^{-\alpha(k)b^{(i)}t})]$, which, according to Eq. (3.2), would describe the evolution of $S(k;t)$ if $b(t)$ remained constant, $b(t) = b^{(i)}$.

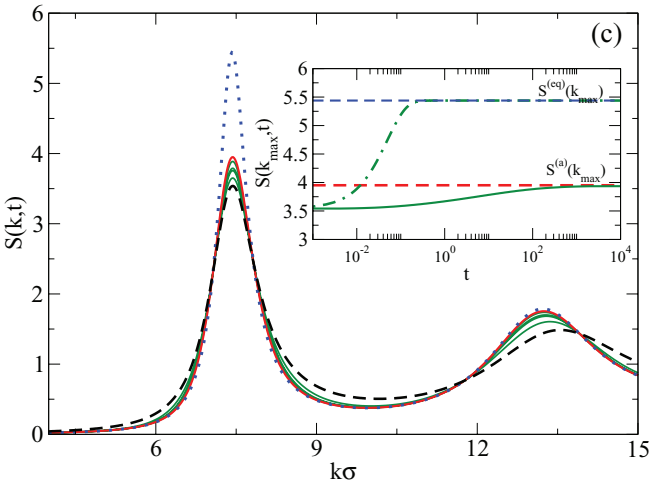

FIG. 11. (Color online) Snapshots of the nonequilibrium evolution of $S(k;t)$ [thin solid (green) lines] corresponding to the isochoric quench at fixed volume fraction $\phi = 0.6$, from $T^{*(i)} = 0.1$ to $T^{*(f)} = 0$. The dashed (black) line is the initial structure factor $S^{(i)}(k)$. The dotted (blue) line is $S_f^{eq}(k)$. The thick solid (red) line is the dynamically arrested asymptotic solution $S^a(k)$ of Eq. (2.3), given by Eq. (5.9). In the inset, the solid line is the maximum of $S(k;t)$ as a function of the evolution time t, and the dashed line is the maximum of $[S^{(i)}(k)e^{-\alpha(k)b^{(i)}t} + [\overline{n}\mathcal{E}^{(f)}(k)]^{-1}(1 - e^{-\alpha(k)b^{(i)}t})]$.

B. Aging of the dynamics

Let us now discuss how the scenario just described manifests itself in the nonequilibrium evolution of the dynamics. We first recall that for each snapshot of the static structure factor $S(k;t)$, the solution of Eqs. (2.7)–(2.11) determines a snapshot at waiting time t of each of the dynamic properties of the system. Thus, the process of dynamic arrest may also be observed, for example, in terms of the t evolution of the self-intermediate scattering function $F_S(k,\tau;t)$ or of the α-relaxation time $\tau_\alpha(k;t)$. In Fig. 12(a) we present a sequence of snapshots of the ISF $F_S(k,\tau;t)$ (thin solid lines), evaluated at the fixed wave vector $k = 7.1$, plotted as a function of correlation time τ, for a sequence of waiting times t after the sudden temperature quench from $T^{*(i)} = 0.1$ to $T^{*(f)} = 0$ at fixed volume fraction $\phi = 0.6$.

In the figure we highlight with the dashed line the initial ISF $F_S(k,\tau;t=0)$. The (arrested) nonequilibrium asymptotic limit $F_S^{(a)}(k,\tau) \equiv \lim_{t\to\infty} F_S(k,\tau;t)$ is indicated by the solid line, whereas the dotted line denotes the inaccessible equilibrium ISF $F_S^{(eq)}(k,\tau)$, i.e., the solution of Eqs. (2.8)–(2.11) in which the final *equilibrium* static structure factor $S^{(eq)}(k;\phi = 0.6,T^{*(f)} = 0)$ (also inaccessible) is employed as static input. We observe that at $t = 0$, $F_S(k,\tau;t)$ shows no trace of dynamic arrest, but as the waiting time t increases, its relaxation time increases as well. In the figure we had to stop at a finite waiting time, but the theory predicts that the ISF $F_S(k,\tau;t)$ will always decay to zero for any finite waiting time t, and continues to evolve forever, yielding always a finite, ever-increasing,

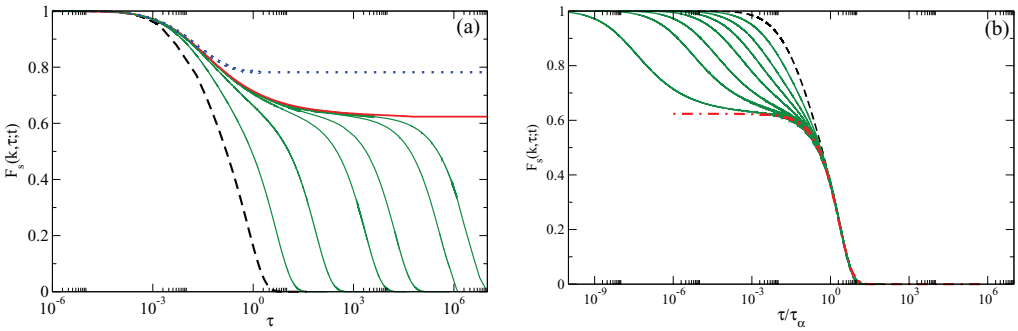

FIG. 12. (Color online) (a) Sequence of snapshots of the intermediate scattering function $F_S(k,\tau;t)$ at $k = 7.1$ [thin solid (green) lines] plotted as a function of correlation time τ for a sequence of values of the waiting time t (=0.25, 5.6, 106, 400, 590, and 1600) after the sudden temperature quench at fixed volume fraction $\phi = 0.6$, from $T^{*(i)} = 0.1$ to $T^{*(f)} = 0$. The dashed line is the initial ISF $F_S(k,\tau;t = 0)$, the thick solid (red) line is the nonequilibrium asymptotic limit $F_S^{(a)}(k,\tau) \equiv F_S(k,\tau;t = \infty)$, and the dotted (blue) line is the expected (but inaccessible) equilibrium ISF corresponding to the hard-sphere system at $\phi = 0.6$. (b) Same sequence of snapshots of $F_S(k,\tau;t)$ plotted as a function of the time t scaled with the α-relaxation time $\tau_\alpha(t)$. The dot-dashed line here is the stretched exponential $0.624 \times \exp[-0.528(t/\tau_\alpha)^{0.82}]$.

α-relaxation time $\tau_\alpha(k;t)$. The relaxation of $F_S(k,\tau;t)$ is characterized by a fast initial decay (β relaxation) to an increasingly better defined plateau, whose height $f_0(k)$ is not determined by the expected equilibrium ISF $F_S^{eq}(k,\tau)$, but by the nonequilibrium asymptotic limit $F_S^{(a)}(k,\tau)$. In other words, $f_0(k)$ is the "true" nonequilibrium nonergodicity parameter $f_S^{(a)}(k) \equiv \lim_{\tau\to\infty} F_S^{(a)}(k,\tau)$.

From this sequence of snapshots of $F_S(k,\tau_\alpha;t)$ we can extract the t evolution of the α-relaxation time $\tau_\alpha(k;t)$ defined in Eq. (4.7). The results allow us to notice one of the main features of the predicted long-τ decay of $F_S(k,\tau;t)$, namely, the long-time collapse of the curves representing $F_S(k,\tau;t)$, corresponding to different evolution times t [like those in Fig. 12(a)], onto the same stretched-exponential curve upon scaling the correlation time τ with the corresponding $\tau_\alpha(k;t)$. In other words, at long times $F_S(k,\tau;t)$ scales as

$$F_S(k,\tau;t) \approx f_0 e^{-a_0(\frac{\tau}{\tau_\alpha(k;t)})^\beta}, \tag{5.15}$$

where f_0 is the height of the plateau of $F_S^{(a)}(k,\tau)$ and $a_0 = 1 + \ln f_0$ [so that $F_S(k,\tau_\alpha;t) = e^{-1}$], and with β being a fitting parameter. This scaling is illustrated in Fig. 12(b) with the sequence of results for $F_S(k,\tau;t)$ in Fig. 12(a) now plotted in this scaled manner, which are then well represented by the stretched-exponential function above, with $f_0 = 0.624$, $a_0 = 0.528$, and $\beta = 0.82$.

The nonequilibrium evolution of the dynamics can be summarized by plotting $\tau_\alpha(k;t)$ as a function of waiting time t. This is done here in Fig. 13, where we plot $\tau_\alpha(t)$ [$\equiv\tau_\alpha(k = 7.1,t)$] as a function of t. The thick dark solid line in Figs. 13(a) and 13(b) derive from the sequence of snapshots of $F_S(k,\tau_\alpha;t)$ in Fig. 12(a), corresponding to the quench at $\phi = 0.6$ with initial temperature $T^{*(i)} = 0.1$. As indicated in these figures, at long waiting times we find that $\tau_\alpha(k;t)$ increases with t according to a power law that is numerically indistinguishable from $\tau_\alpha(t) \propto t^\eta$ with $\eta \approx 1.83$. In other words, the present theory predicts, taking into account Eq. (5.6), that at long waiting times, $\tau_\alpha(k;t)$ diverges with t with the same power law as $b^{-1}(t)$.

Besides these results, Fig. 13(a) also presents theoretical results for two additional quench programs that differ only in the initial temperature, namely, $T^{*(i)} = 0.05$ and $T^{*(i)} = 0.01$. These three initial temperatures lie above the dynamic arrest transition temperature $T^{*(a)}(\phi)$ corresponding to the isochore

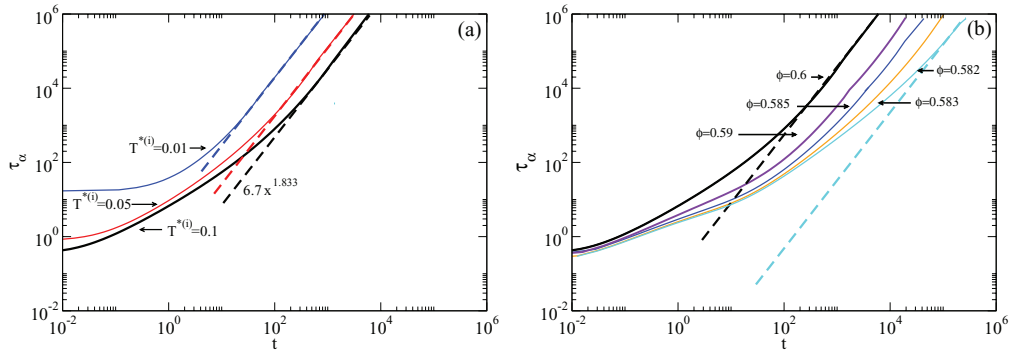

FIG. 13. (Color online) Waiting-time dependence of the α-relaxation time $\tau_\alpha(t;T^{*(i)},\phi)$ (defined in the text) after the sudden temperature quench at fixed volume fraction ϕ, from an initial temperature $T^{*(i)}$ to a final temperature $T^{*(f)} = 0$. In (a) we present the results for the initial temperatures $T^{*(i)} = 0.1$, 0.05, and 0.001 at the same volume fraction $\phi = 0.6$. In (b) we fix the initial temperature $T^{*(i)} = 0.1$ and present results for $\phi = 0.6$ and other volume fractions. The dashed lines indicate the asymptotic power law $\tau_\alpha(t) \propto At^x$ that fits the results in the indicated regimes.

$\phi = 0.6$, which is $T^{*(a)}(\phi = 0.6) = 0.004$. The first feature to notice is that the detailed waiting time dependence of τ_α at short times may be strongly quench-dependent, but the asymptotic power law $\tau_\alpha(t) \propto t^\eta$ with the exponent $\eta \approx 1.83$ is independent of the initial temperature $T^{*(i)}$. Complementing this information, Fig. 13(b) describes the dependence of the evolution of $\tau_\alpha(t; T^{*(i)}, \phi)$ on the value of the volume fraction ϕ at which these isochoric processes occur, assuming that each of them start and end at the same initial and final temperatures, $T^{*(i)} = 0.1$ and $T^{*(f)} = 0$. The main feature to notice in these results is that the long-time asymptotic growth of $\tau_\alpha(t; \phi)$ with waiting time t is also characterized by the power law $\tau_\alpha(t) \propto t^{1.83}$.

VI. CROSSOVER FROM EQUILIBRATION TO AGING

Of course, one could continue describing the predictions of the NE-SCGLE theory regarding the detailed evolution of each relevant structural and dynamic property of the glass-forming system along the process of equilibration or aging. At this point, however, we would like to unite the main results of the previous two sections in a single integrated scenario that provides a more vivid physical picture of the predictions of the present theory. With this intention, in Fig. 14(a) we have put together the results for the isochoric evolution of $\tau_\alpha(t; \phi)$ previously presented in Figs. 8(b) and 13(b), corresponding to the quench at fixed volume fraction ϕ, from an initial temperature $T^{*(i)} = 0.1$ to a final temperature $T^{*(f)} = 0$, for volume fractions ϕ smaller and larger than $\phi^{(a)} = 0.582$.

Displaying together these results allows us to have a richer and more comprehensive scenario of the transition from equilibration processes to aging processes in the soft-sphere glass-forming liquid, discussed separately in the previous two sections. According to the NE-SCGLE theory, the dynamic arrest transition is, in principle, a discontinuous transition, involving the abrupt passage from one pattern of evolution (equilibration) to the other (aging) when the control parameter ϕ crosses the singular value $\phi^{(a)} = 0.582$. The discontinuous nature of this kinetic transition is rooted in the abrupt transition contained in the *equilibrium* version of the SCGLE theory, which actually predicts the existence and location of the dynamic arrest transition line (see Fig. 13). The zero-temperature limit of this transition line corresponds to the critical volume fraction $\phi^{(a)} = 0.582$. Thus, the evolution of the system after the temperature quench from an initial temperature $T^{*(i)} = 0.1$ to a final temperature $T^{*(f)} = 0$ is dramatically different if the volume fraction of the isochoric process is smaller or larger than this critical volume fraction.

However, in order to actually witness this dramatic difference, we would have to perform observations at volume fractions infinitesimally closer to $\phi^{(a)}$ and within an evolution time window much larger (in fact, infinite) than in any real experiment or simulation. In fact, what we would like to illustrate now is that the experimental observation of the consequences of this theoretically predicted singularity will be blurred by this unavoidable finiteness of the time window of any experimental observation. To see this, let us display the same information presented in Fig. 14(a), which plots $\tau_\alpha(t; \phi)$ as a function of t for a sequence of volume fractions ϕ, in a complementary format. This is done in Fig. 14(b), which plots $\tau_\alpha(t; \phi)$ as a function of ϕ for a sequence of waiting times t.

The main feature to notice in each of the curves corresponding to a fixed waiting time t, is that one can distinguish two regimes in volume fraction, namely, the low-ϕ (equilibrated) regime and the high-ϕ (nonequilibrated) regime, separated in a continuous fashion, and not as an abrupt transition, by a crossover volume fraction $\phi^{(c)}(t)$. Focusing, for example, on the results corresponding to $t = 10^3$, we notice that $\phi^{(c)}(t = 10^3) \approx 0.57$. In Fig. 14(b) we have highlighted the crossover points $\phi = \phi^{(c)}(t)$, $\tau_\alpha(t, \phi) = \tau_\alpha^{eq}(\phi^{(c)})$, corresponding to each waiting time t considered. We observe that the resulting crossover volume fraction $\phi^{(c)}(t)$ first increases rather fast with t, but then slows down considerably, reaching a theoretical maximum crossover volume fraction, $\lim_{t\to\infty} \phi^{(c)}(t)$, given by $\phi^{(a)} = 0.582$, as indicated in the inset of the figure.

The scenario illustrated by Fig. 14(b) has additional physical implications. Although it is impossible to witness the infinite-time consequences of the theoretically predicted singular dynamic arrest transition, it is important to stress

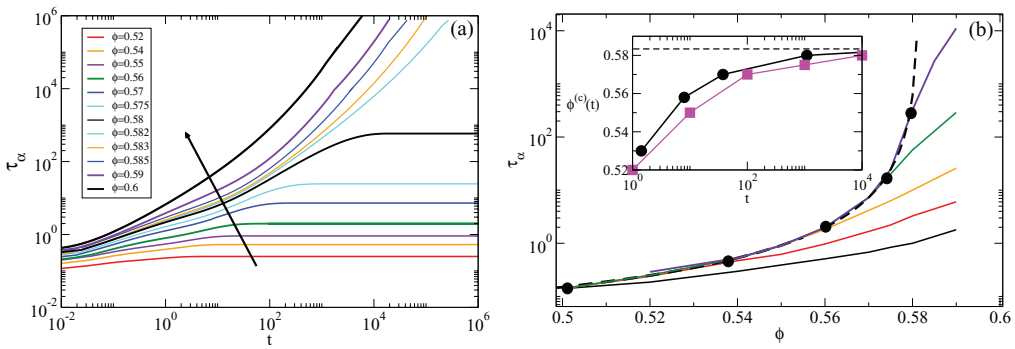

FIG. 14. (Color online) (a) Waiting time dependence of the α-relaxation time $\tau_\alpha(t; \phi)$ for a sequence of fixed volume fractions (the arrow indicates increasing ϕ). (b) ϕ dependence of the α-relaxation time $\tau_\alpha(t; \phi)$ for the sequence of fixed waiting times $t = 10^0, 10^1, 10^2, 10^3$, and 10^4 (from bottom to top). The dashed line is $\tau_\alpha^{eq}(\phi) \equiv \lim_{t\to\infty} \tau_\alpha(t; \phi)$, which is the *equilibrium* α-relaxation time of the hard-sphere system, predicted by the equilibrium SCGLE theory. The solid circles highlight the crossover points $(\phi^{(c)}(t), \tau_\alpha^{eq}(\phi^{(c)}))$ for each waiting time t shown. The inset of (b) shows the evolution of the crossover volume fraction $\phi^{(c)}(t)$ predicted by the NE-SCGLE theory (solid line) and determined in the simulations of Ref. [8] (solid squares).

that its finite-time predictions, such as those illustrated in this figure, could be corroborated by performing measurements at *intentionally* finite, accessible waiting times. It is thus important to test if these predictions make sense by comparing them with available experimental or simulation data. In this regard, we can advance that the picture that emerges from the predicted dependence of $\tau_\alpha(t;\phi)$ on waiting time and volume fraction, just illustrated in Fig. 14, is fully consistent with the most relevant qualitative features observed in a simulation experiment consisting precisely of the equilibration of a hard-sphere liquid, initially prepared in a nonequilibrium state [8]. In fact, such simulation experiment was originally inspired by the theoretical scenario offered by the present nonequilibrium theory. To have an idea of the level of agreement, in the inset of Fig. 14(b) we have included the simulation data for the evolution of the crossover volume fraction $\phi^{(c)}(t)$ with waiting time reported in Ref. [8]. The comparison between the predicted full dependence of $\tau_\alpha(t;\phi)$ on volume fraction at various waiting times [displayed in Fig. 14(b)] and the corresponding simulation data in Fig. 2 of Ref. [8] turns out to exhibit the same degree of agreement, as can be observed in Fig. 3(c) of Ref. [40]. In later work, however, we shall analyze in detail other aspects of the systematic comparison between the predictions of the NE-SCGLE theory and available simulation results, which does confirm this general qualitative agreement.

Another manner to test the predictive power of the present theory is to exhibit its relevance in interpreting the wealth of available experimental data on the equilibration and aging processes in glass-forming liquids and glasses. Many such experimental data are very well fitted by phenomenological models and theories, and it is interesting to see if the predictions of our theory are consistent with the main features and trends described by the most successful of these phenomenological models. For example, the Tool-Narayanaswamy model [41,42], summarized in recent papers by T. Hecksher *et al.* [43] and by Richert [44], interpret aging in terms of a so-called internal (or "material") time. These models, which are commonly used in industry for predicting aging effects [45], describe the highly nonlinear aging processes in terms of a formally linear convolution integral. Although the resulting description turns out to capture the experimentally observed behavior, the fundamental reason for its success is not yet fully understood. In fact, one important open question is if the very existence of an internal clock has a sound physical basis, or if it is just a convenient mathematical construction.

In this context, it is important to notice that the structure of the NE-SCGLE equations is indeed consistent with the notion of an internal clock. To see this, let us notice that the variable $u(t)$, defined in Eq. (2.6) of our paper in terms of the dimensionless mobility $b(t)$, plays the role of the dimensionless reduced time (or inner clock), denoted as $\widetilde{t}(t)$ in Eq. (4) of Hecksher *et al.* or as $\zeta(t)$ in Eq. (1) of Richert's paper. Similarly, our dimensionless mobility $b(t)$ can be identified with the structural clock rate $\gamma(t)$ of Hecksher *et al.*, which is denoted as $1/\tau(t)$ in Richert's paper. In addition, it is not difficult to see that our time-evolution equation for the nonequilibrium static structure factor $S(k;t)$ [Eq. (2.3) of our paper] has the same mathematical structure of the generic nonlinear equation $dX_t/dt = -(X_t - X_\infty)/\tau(X_t)$ which, according to Richert, describes aging. As a result, the formal solution for $S(k;t)$ in Eq. (2.4) of our paper has the same structure as the generic solution in Eq. (2) of Richert's paper, namely, $X_t = X_\infty + (X_0 - X_\infty)\exp[-\int_0^t dt'/\tau(t')]$. Discussing the detailed implications of these mathematical similarities must, however, be the subject of a separate report.

VII. CONCLUDING REMARKS

In summary, in this work we have started the systematic exploration of the predicted NE-SCGLE scenario of the irreversible isochoric evolution of a soft-sphere glass-forming liquid whose temperature is suddenly quenched from its initial value $T^{(i)}$ to a final value $T^{(f)} = 0$. As we explained here, the response falls in two mutually exclusive possibilities: Either the system will reach its new equilibrium state within an equilibration time $t^{eq}(\phi)$ that depends on the fixed volume fraction ϕ, or the system ages forever in the process of becoming a glass.

In the first case the equilibrium α-relaxation time $\tau_\alpha^{eq}(\phi)$, and the equilibration time $t^{eq}(\phi)$ needed to reach thermodynamic equilibrium, are predicted to remain finite for volume fractions smaller than a critical value $\phi^{(a)} \approx 0.582$, but as ϕ approaches this hard-sphere dynamic-arrest volume fraction, both characteristic times will diverge and will remain infinite for $\phi \geqslant \phi^{(a)}$. Although it is intrinsically impossible to witness the actual predicted divergence, the theory makes distinct predictions regarding the transient nonequilibrium evolution occurring within experimentally reasonable waiting times t, which could, thus, be compared with realizable experiments or simulations.

This applies even more to the predictions regarding the complementary regime, $\phi \geqslant \phi^{(a)}$, in which the system, rather than ever reaching equilibrium, is predicted to age forever. As discussed in the previous section, under these circumstances the long-time asymptotic limit of $S(k;t)$ will no longer be the expected equilibrium static structure factor $S^{(eq)}(k)$, but the nonequilibrium, but well-defined, dynamically arrested static structure factor $S^{(a)}(k)$. Furthermore, $S(k;t)$ is predicted to approach $S^{(a)}(k)$ in a much slower fashion (a power law), in contrast with the exponential-like manner in which $S(k;t)$ approaches $S^{(eq)}(k)$ when the system equilibrates.

Putting together the two regimes just described, we have presented the predicted scenario for the crossover from equilibration to aging. As discussed in the previous section, the discontinuous and singular behavior predicted by the (MCT or SCGLE) theories is intrinsically unobservable in practice, due to the finiteness of the time windows of experimental measurements. This forces the discontinuous dynamic arrest transition to appear as a blurred crossover, which may depend on the protocol of the experiment and of the measurements. Testing these predictions by systematically comparing them with available experimental or simulation data is an issue that we leave for future studies, since the main purpose here was to provide the details of the methodologies needed to solve the equations that define the NE-SCGLE and to illustrate its use with the application to the specific system and processes considered here.

Nevertheless, it is important to notice that a considerable conceptual difference may arise in the interpretation of specific

simulation data if one adopts the perspective provided by the present theory, compared to more conventional perspectives. For example, Berthier and Witten [46] find that their computer simulation dynamic data "show evidence of an avoided mode-coupling singularity near $\phi_{MCT} \approx 0.592$" and determine a singular volume fraction $\phi_0 \approx 0.635$ through the apparent divergence of their measured relaxation times (which they assume to correspond to fully equilibrated systems). From our perspective, however, it is not difficult to convince oneself that our singular volume fraction $\phi_{HS}^{(a)} = 0.582$ is conceptually identical to what Berthier and Witten (and most anyone) refer to as ϕ_{MCT}, and that the dynamic arrest transition line in Fig. 1 of our paper corresponds to what Berthier and Witten refer to as the mode-coupling transition line, $T_{MCT}(\phi)$ in their Fig. 2. The differences are that we refer to the TLJ liquid, rather than to harmonic spheres, and that we employ the nonequilibrium extension (NE-SCGLE) of the SCGLE theory instead of conventional MCT (whose nonequilibrium version is not yet available).

One should not confuse, however, the avoided singularity at $\phi_{HS}^{(a)} = 0.582$ with the unavoidable singularity of *mechanical* nature to jammed, stable packings of hard spheres found when its volume fraction ϕ approaches its random close packing (RCP) value $\phi_{RCP} = 0.637$ [47]. The dynamic arrest singularity predicted by MCT (and by our *equilibrium* SCGLE theory) can be said to be the amorphous kinetic version of the thermodynamic equilibrium crystallization transition. Thus, when the volume fraction of an equilibrated hard-sphere system reaches its melting point $\phi^{(m)} \approx 0.54$, all the constituent particles are dynamically arrested, in the sense that the equilibrium long-time self-diffusion coefficient D_L^{eq} vanishes. Thermal motion, however, keeps the particles rattling within the finite localization length γ allowed by their rigid cage of neighbors. This length decreases with further compression down to $\gamma = 0$, a limiting value that must be the signature of the transition from localized thermal motion to collective mechanically jammed conditions, expected to occur in the monodisperse hard-sphere system at the hexagonal close packing (HCP) volume fraction $\phi_{HCP} \approx 0.74$. Thus, in the interval $\phi^{(m)} \leqslant \phi < \phi_{HCP}$, the state of the equilibrium crystal is characterized by $D_L^{eq} = 0$ and $\gamma > 0$.

In contrast, in sufficiently polydisperse samples, the HS system remains in its ergodic liquid state well beyond the freezing volume fraction $\phi^{(f)} = 0.494$. The resulting metastable states are characterized by $D_L^{eq} > 0$, $\tau_\alpha^{eq} < \infty$, and $\gamma = \infty$. MCT and the equilibrium SCGLE theory provide the equilibrium value of these dynamic order parameters and predict a transition to dynamically arrested states characterized by the values $D_L^{eq} = 0$, $\tau_\alpha^{eq} = \infty$, and $\gamma > 0$ at a volume fraction $\phi^{(a)}$ (which the SCGLE theory locates at $\phi^{(a)} = 0.582$). An ideal material with these properties in the interval $\phi^{(a)} \leqslant \phi < \phi_{RCP}$ is an *equilibrium glass*, whose experimental observation is impossible since its equilibration waiting time t_w^{eq} is as infinite as τ_α^{eq}. Nevertheless, just like the equilibrium HS crystal becomes jammed at ϕ_{HCP}, this equilibrium glass must also become mechanically jammed at its RCP volume fraction $\phi_{RCP} = 0.637$, at which the localization length γ should be expected to vanish. Thus, the fundamental difference between dynamic arrest and jamming is that dynamic arrest is characterized by the passage of γ from infinity to a finite value, whereas jamming is expected to occur when $\gamma \to 0$.

Let us clarify that, according to our theory, the *measured* α relaxation time $\tau_\alpha(t_w)$, experimentally determined within the finite equilibration or waiting times of a given experiment or simulation, may always remain finite within finite observation times, as illustrated in Fig. 14(b) of our paper. It is the *equilibrium* α relaxation time τ_α^{eq} that falls out of the reach of finite-time measurements as soon as ϕ reaches the value $\phi^{(a)}$. Thus, any real experimental measurement, performed within finite experimental times will only register a blurred picture, or the "vestige," of the predicted divergence (i.e., the MCT avoided divergence). The main contribution of the present paper is, hence, this proposed physical meaning of the avoided singularity at $\phi^{(a)}$ and the mechanisms for its avoidance. As indicated at the end of the previous section, we can say that the resulting scenario is consistent with the most relevant qualitative features observed in the simulation experiment of the equilibration of the hard-sphere liquid [8].

In future work we shall establish a more direct contact with those simulation results, and with other simulation or experimental data, but in the meantime, it will also be interesting to interrogate the NE-SCGLE theory on the variations of the scenario just described, when the system and conditions employed here are modified. For example, one may be interested in understanding how this scenario might change when the protocol of the quench is modified. Other questions may refer to the dependence of this scenario on the particular class of model system and interactions (involving here only soft repulsions), particularly when attractive forces are incorporated. The answer to these questions will surely use the methods and experience developed in the presented work and will be the subject of future research.

Let us finally mention that one of the most important contributions of the present work is to pose the question whether current experiments and simulations of dense particulate systems are able to equilibrate the system at packing fractions above 58%. This is an important issue, given the fact that there are simulation results in the literature which claim that well-equilibrated repulsive liquids can be obtained in molecular dynamics simulations at packing fractions near random close packing (see, e.g., Ref. [46] and references therein). In order to have additional independent elements to discuss this issue, in the inset of Fig. 14(b) we have referred to the simulations of hard spheres performed in Ref. [8], in which the structural relaxation time $\tau_\alpha(t;\phi)$ was measured as a function of waiting time and packing fraction.

We must caution, however, that these simulations, like any other, are limited to a finite time window (in this case they only include relaxation times up to 10^5 in units of the molecular collision time $\sigma\sqrt{M/k_BT}$). This apparent saturation of the crossover volume fraction $\phi^{(c)}(t)$ to $\phi^{(a)} \approx 0.582$, shown in the inset of Fig. 14(b), is thus backed only by the simulation data in this limited time window. Hence, the possibility exists that future simulations carried out in much larger time windows might exhibit deviations from the scenario proposed by the present theory. This would demonstrate that this theory misses some crucial ingredient that would allow the equilibration of the HS system at volume fractions above

0.582 and would move the divergence of equilibration times closer to random close packing. Simulations to date, however, have not definitively answered this important question, and, hence, extending further the time window will surely illuminate the discussion around this central issue. In the meantime, it would also be desirable to relax some of the obvious limitations of the present theory, such as the absence of static and dynamic heterogeneities and the underlying approximation of local stationarity, as we intend to do in the future.

ACKNOWLEDGMENTS

The authors acknowledge an anonymous referee for drawing our attention to Refs. [41–45]. We also acknowledge M. A. Ojeda-López, P. Mendoza-Méndez, L. López-Flores, and E. Lázaro-Lázaro for helpful discussions. This work was supported by the Consejo Nacional de Ciencia y Tecnología (CONACYT, México), through Grants No. 182132 and No. 132540 and by the Fondo de Recursos Concurrentes UASLP (Grant No. C11-FRC-09-06.06).

[1] H. Callen, *Thermodynamics* (Wiley, New York, 1960).
[2] D. A. McQuarrie, *Statistical Mechanics* (Harper & Row, New York, 1973).
[3] S. R. de Groot and P. Mazur, *Non-equlibrium Thermodynamics* (Dover, New York, 1984).
[4] J. Keizer, *Statistical Thermodynamics of Nonequilibrium Processes* (Springer-Verlag, Berlin, 1987).
[5] G. Lebon, D. Jou, and J. Casas-Vázquez, *Understanding Non-equilibrium Thermodynamics Foundations, Applications, Frontiers* (Springer-Verlag, Berlin, Heidelberg, 2008).
[6] C. A. Angell, Science **267**, 1924 (1995).
[7] P. G. Debenedetti and F. H. Stillinger, Nature (London) **410**, 359 (2001).
[8] G. Pérez-Angel, L. E. Sánchez-Díaz, P. E. Ramírez-González, R. Juárez-Maldonado, A. Vizcarra-Rendón, and M. Medina-Noyola, Phys. Rev. E **83**, 060501(R) (2011).
[9] K. Kim and S. Saito, Phys. Rev. E **79**, 060501(R) (2009).
[10] A. Latz, J. Phys.: Condens. Matter **12**, 6353 (2000).
[11] W. Götze, in *Liquids, Freezing and Glass Transition*, edited by J. P. Hansen, D. Levesque, and J. Zinn-Justin (North-Holland, Amsterdam, 1991).
[12] W. Götze and L. Sjögren, Rep. Prog. Phys. **55**, 241 (1992).
[13] W. Götze and E. Leutheusser, Phys. Rev. A **11**, 2173 (1975).
[14] W. Götze, E. Leutheusser, and S. Yip, Phys. Rev. A **23**, 2634 (1981).
[15] B. Berne, in *Statistical Mechanics, Part B: Time-dependent Processes*, edited by B. Berne (Plenum, New York, 1977).
[16] P. De Gregorio *et al*., Physica A **307**, 15 (2002).
[17] L. Yeomans-Reyna and M. Medina-Noyola, Phys. Rev. E **64**, 066114 (2001).
[18] L. Yeomans-Reyna, H. Acuña-Campa, F. de Jesús Guevara-Rodríguez, and M. Medina-Noyola, Phys. Rev. E **67**, 021108 (2003).
[19] M. A. Chávez-Rojo and M. Medina-Noyola, Physica A **366**, 55 (2006).
[20] M. A. Chávez-Rojo and M. Medina-Noyola, Phys. Rev. E **72**, 031107 (2005); **76**, 039902 (2007).
[21] P. E. Ramírez-González *et al*., Rev. Mex. Fis. **53**, 327 (2007).
[22] L. Yeomans-Reyna, M. A. Chávez-Rojo, P. E. Ramírez-González, R. Juárez-Maldonado, M. Chávez-Páez, and M. Medina-Noyola, Phys. Rev. E **76**, 041504 (2007).
[23] R. Juárez-Maldonado, M. A. Chávez-Rojo, P. E. Ramírez-González, L. Yeomans-Reyna, and M. Medina-Noyola, Phys. Rev. E **76**, 062502 (2007).
[24] R. Juárez-Maldonado and M. Medina-Noyola, Phys. Rev. Lett. **101**, 267801 (2008).
[25] L. E. Sánchez-Díaz, A. Vizcarra-Rendón, and R. Juárez-Maldonado, Phys. Rev. Lett. **103**, 035701 (2009).
[26] P. E. Ramírez-González and M. Medina-Noyola, Phys. Rev. E **82**, 061503 (2010).
[27] P. E. Ramírez-González and M. Medina-Noyola, Phys. Rev. E **82**, 061504 (2010).
[28] G. Brambilla, D. El Masri, M. Pierno, L. Berthier, L. Cipelletti, G. Petekidis, and A. B. Schofield, Phys. Rev. Lett. **102**, 085703 (2009).
[29] D. El Masri, G. Brambilla, M. Pierno, G. Petekidis, A. B. Schofield, L. Berthier, and L. Cipelletti, J. Stat. Mech. Theory Exp. (2009) P07015.
[30] U. Marini Bettolo Marconi and P. Tarazona, J. Chem. Phys. **110**, 8032 (1999); J. Phys.: Condens. Matter **12**, A413 (2000).
[31] L. López-Flores *et al*., Europhys. Lett. **99**, 46001L (2012).
[32] L. López-Flores, L. L. Yeomans-Reyna, M. Chávez-Páez, and M. Medina-Noyola, J. Phys.: Condens. Matter **24**, 375107 (2012).
[33] H. C. Andersen, J. D. Weeks, and D. Chandler, Phys. Rev. A **4**, 1597 (1971).
[34] L. Verlet and J. J. Weis, Phys. Rev. A **5**, 939 (1972).
[35] J. K. Percus and G. J. Yevick, Phys. Rev. **110**, 1 (1957).
[36] J. P. Hansen and I. R. McDonald, *Theory of Simple Liquids* (Academic Press, San Diego, 1976).
[37] R. Evans, Adv. Phys. **28**, 143 (1979).
[38] P. E. Ramírez-González, L. López-Flores, H. Acuña-Campa, and M. Medina-Noyola, Phys. Rev. Lett. **107**, 155701 (2011).
[39] P. G. de Gennes, Physica **25**, 825 (1959).
[40] L. E. Sánchez-Díaz, P. E. Ramírez-González, and M. Medina-Noyola, AIP Conf. Proc. **1518**, 28 (2012).
[41] A. Q. Tool, J. Am. Ceram. Soc. **29**, 240 (1946).
[42] O. S. Narayanaswamy, J. Am. Ceram. Soc. **54**, 491 (1971).
[43] T. Hecksher, N. B. Olsen, K. Niss, and J. C. Dyre, J. Chem. Phys. **133**, 174514 (2010).
[44] R. Richert, Phys. Rev. Lett. **104**, 085702 (2010).
[45] L. Hornboll, T. Knusen, Y. Yue, and X. Guo, Chem. Phys. Lett. **494**, 37 (2010).
[46] L. Berthier and T. A. Witten, Phys. Rev. E **80**, 021502 (2009).
[47] L. Woodcock, J. Phys. Chem. B **116**, 3735 (2012).